January 1973

Head Losses Due to Ring-Tite Filament Wound Elbows and Tees and Frictional Losses in Pipes of Polyvinylchloride

Roland W. Jeppson

HEAD LOSSES DUE TO RING-TITE FILAMENT WOUND ELBOWS AND TEES AND FRICTIONAL LOSSES IN PIPES OF POLYVINYLCHLORIDE

by

Roland W. Jeppson

Supported by

Johns-Manville
Research & Engineering Center
Denver, Colorado

Utah Water Research Laboratory
College of Engineering
Utah State University
Logan, Utah 84322

February 1973

PRWG-132

ACKNOWLEDGMENTS

Special recognition is due Scott McAllister and Dennis Cropper, senior engineering students at USU, for their very able assistance during the course of this research. These two men obtained the laboratory data in the report, and the results in the report depended heavily upon the good professional judgment of these individuals for the quality of data obtained.

The head losses in the 6 x 6 x 6-inch tee were also measured with the tee operating to separate the flow coming into one of the "straight through" branches into two outflows. The head loss coefficients which measure the head loss between the two "straight through" branches plot against Reynolds number as a straight line on log-log paper. The head loss coefficients which measure the head loss between the "straight through" inlet and the branch 90° therefrom are larger than the previous coefficients and tend toward constant values at the higher Reynolds number of the tests. A summary of these head loss coefficients is given on Fig. 15.

In addition the head losses in the 6 x 6 x 6-inch tee were measured with the flow coming into two branches of the tee and being combined into a single outflow from one branch. The combined outflow was passed through one of the "straight through" branches with the inflows coming into the other "straight through" branch and the branch at 90° therefrom. In this mode of operation the tee becomes a simple two branch manifold. The several head loss coefficients for this mode of operation to combine the flows are summarized on Fig. 16, but also vary with Reynolds number.

TABLE OF CONTENTS

LIST OF TABLES

LIST OF TABLES (CONTINUED)

LIST OF FIGURES

LIST OF FIGURES (CONTINUED)

INTRODUCTION

This report describes the collection and analyses of data used to determine frictional head losses in pipes and also to determine head losses due to an elbow and two tees in various modes of operation. The basic fluid principles governing frictional losses in pipes is well known, but for the sake of completeness this introduction will briefly give these essential equations for computing frictional losses in pipe flows, and will also describe the phenomena of "minor losses" due to elbows and tees.

Pipe Friction

The most fundamentally sound method for computing head losses (or pressure drops) due to fluid friction from flows in pipes is by means of a relatively simple equation which has become known as the Darcy-Weisbach equation. The Darcy-Weisbach equation is,

$$h_f = \frac{\Delta P}{\gamma} = f \frac{L}{d} \frac{V^2}{2g} \quad . \quad . \quad . \quad . \quad . \quad . \quad . \quad . \quad . \quad (1)$$

in which f is a dimensionless friction factor whose determination is discussed below, L is the length of pipe (ft), d is the pipe diameter (ft) and V is the average velocity of flow (ft/sec), and γ is the specific weight of the fluid (lb/ft^3).

The Moody diagram is commonly used to obtain the friction factor, if hand computations are used. For computer use it is better to use equation representing the information on the Moody diagram. These equations are:

(a) For laminar flow defined by the Reynolds number $R_e = Vd/\nu < 2100$,

$$f = \frac{64}{R_e} \quad . \quad . \quad . \quad . \quad . \quad . \quad . \quad . \quad . \quad . \quad . \quad . \quad (2)$$

(b) For hydraulically smooth flow,

$$f = \frac{.316}{R_e^{.25}} \quad \text{for } 2100 < R_e < 10^5 \quad . \quad . \quad . \quad . \quad . \quad . \quad (3)$$

(explicit equation but applicable to a limited range of Reynolds numbers).

$$\frac{1}{\sqrt{f}} = 2 \log_{10} (R_e \sqrt{f}) - 0.8 \quad \text{for } R_e > 2100 \quad . \quad . \quad . \quad (4)$$

(c) Transition between hydraulically smooth and wholly rough flow,

$$\frac{1}{\sqrt{f}} = -2 \log_{10} \left(\frac{e/d}{3.7} + \frac{2.52}{R_e \sqrt{f}} \right) = 1.14 - 2 \log_{10} \left(\frac{e}{d} + \frac{9.35}{R_e \sqrt{f}} \right)$$

$$. \quad . \quad . \quad . \quad . \quad . \quad . \quad (5)$$

(d) Wholly rough flow,

$$\frac{1}{\sqrt{f}} = 1.14 - 2 \log_{10} \frac{e}{d} \quad . \quad . \quad . \quad . \quad . \quad . \quad . \quad . \quad . \quad . \quad (6)$$

In the above equations R_e is Reynolds number, i.e. $R_e = Vd/\nu$ (ν is the kinematic viscosity ft^2/sec), and e is the equivalent roughness of the pipe wall material.

In general the friction factor f is a function of Reynolds number and the relative roughness of the pipe, e/d, as Eqs. 2 through 6 indicate. More specifically, however, for laminar flows, f is only a function of Reynolds number, and for wholly rough flows is only a function of the relative roughness, e/d. If a flow is hydraulically smooth, the material roughnesses are embedded well within the laminar sublayer, and consequently f is only a function of Reynolds number. Consequently, only in the transition region between hydraulically smooth and wholly rough flow (Eq. 5) is the friction factor a function of both Reynolds number and the relative roughness of the pipe wall e/d. In other regions the functional relationship changes from one of these variables to the other. In the subsequent analyses of the data by the computer, Eqs. 4

through 6 have been used. In solving the implicit equations (Eqs. 4 and 5) the Newton-Raphson iterative method has been used.

Minor Losses

The loss of fluid energy due to elbows, tees, valves and other pipe fittings are termed "minor losses" even though they may contribute significantly to the total loss, particularly for flows in short lengths of pipes. Theory for describing minor losses has not been developed from basic fluid principles as has frictional losses in pipes, primarily because the flow becomes three-dimensional with separation, added turbulence, and secondary motions occurring, all of which cannot be described mathematically with sufficient precision to be useful in determining energy losses. Consequently, these losses are commonly given by an equation of the form

$$h_L = C_L \frac{V^2}{2g} \quad . \quad . \quad . \quad . \quad . \quad . \quad . \quad . \quad . \quad . \quad . \quad (7)$$

in which the head loss coefficient C_L is an empirical constant determined from tests. For enlargements the average velocity of the flow V is replaced by the difference in velocities at the two sections. In using Eq. 7 the "no-length" concept is used. This concept considers the loss due to the fitting to be that only in excess of the loss produced by a straight pipe of equal length.

If the minor loss is due primarily to separation with the accompanying eddy and turbulent energy dissipation, the added loss is confined principally to the flow in the vicinity of the fitting. Particularly for smooth bends with large radii of curvature, however, a double spiral secondary motion is set up at the bend as the higher velocity core fluid moves outward under the action of the centrifugal forces at the bend and displaces the slower moving fluid near the pipe walls to the inside of the bend. This secondary spiral motion exists in the pipe downstream

from the bend for 50 to 100 pipe diameters until viscous resistance eventually eliminates it. The velocity caused by this secondary motion is superimposed on the main axial velocity of the flow and contributes to frictional losses in excess of those that would exist without the secondary motion. Consequently, the head loss due to a smooth bend actually occurs principally in the pipe downstream from the bend.

Separation occurs in most commercial elbows so that much of the loss due to them is confined to the vicinity of the elbow, but they can also create secondary motions which can persist some distance downstream of the elbow.

Even though the loss of energy due to pipe fittings has been studied by engineers and applied scientists for more than a century, there appears to be a deficiency of data which can be used to determine loss coefficients at junctions that either separate flow from one pipe into two pipes or combine flows from two or more pipes into a single discharge pipe, such as tees do. Blaisdell and Manson (1963 and 1967) carried out extensive tests on different combinations of pipe junctions primarily for application to tile drainage systems. The head losses due to some tees have been measured by Giesecke et al. (1932) and Hoopes (1948); and Jamison (1971) studied losses in the laminar flow range for both combined and separated flows. Ruus (1970) tested the influence of the angle of bifurcation on the head losses in lucite wyes. Some of the tests done on hydraulic manifolds gives some insight into tees operating in the mode of combining flows from two sources (see McNown (1952), Amorocho and Johannas (1971), and Jeppson, Clyde and Kincaid (1972 and 1973)).

OBJECTIVES

The collection of laboratory data, and the analyses of this data was with the following objectives in mind.

1. Determination of the frictional head loss coefficients in 6-inch PERMASTRAN® pipe.

2. Determination of the frictional head loss coefficients in 4-inch PERMASTRAN® pipe.

3. Determination of the head loss due to a 6-inch RING-TITE filament-wound 90° elbow.

4. Determination of the head loss due to a 6 x 6 x 6-inch RING-TITE filament-wound tee operating with flow entering one of the "straight through" branches and the entire flow leaving in a direction 90° therefrom. The 20-foot long pipe fitted into the other "straight through" branch which was plugged at its end causing the described flow as illustrated in Fig. 1 below.

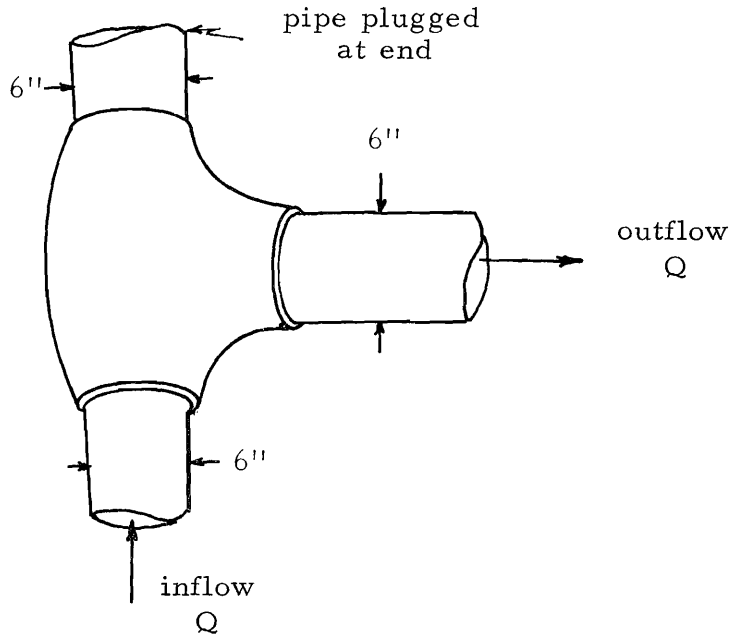

Fig. 1. Operation of the 6 x 6 x 6-inch RING-TITE filament wound tee acting to turn the entire flow through 90-degrees.

5. Determination of the head loss due to a 6 x 6 x 4-inch RING-TITE filament wound tee operating with the flow entering one of the "straight through" branches and the entire flow leaving in a direction 90° therefrom through the 4-inch branch of the tee as illustrated in Fig. 2. The 6-inch 20-foot long pipe fitted into the other "straight through" branch was plugged at its end.

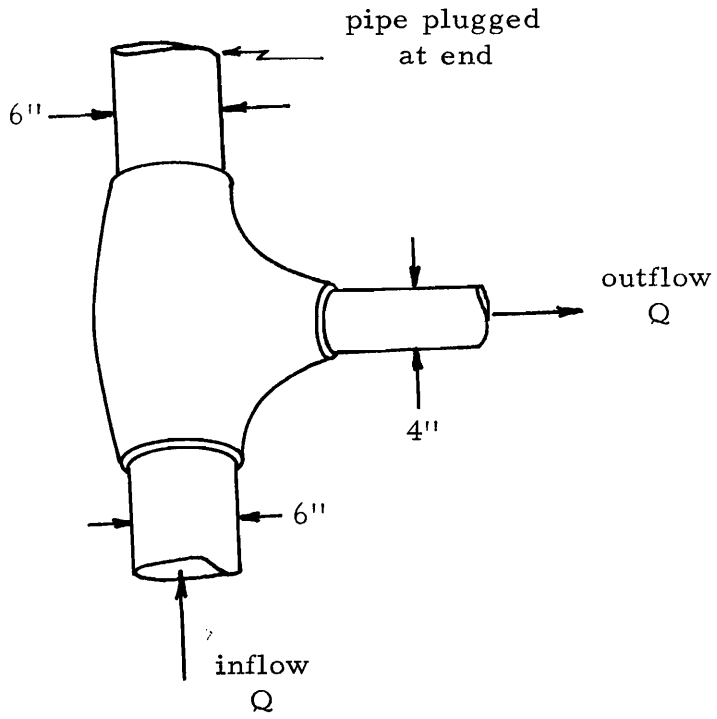

Fig. 2. Operation of 6 x 6 x 4-inch RING-TITE filament wound tee acting to turn the flow through 90-degrees.

6. Determination of the head losses due to a 6 x 6 x 6-inch RING-TITE filament-wound tee operating to separate the inflow which comes into one of the "straight through" branches into flow out of the other "straight through" branch and the branch 90° therefrom as illustrated in Fig. 3.

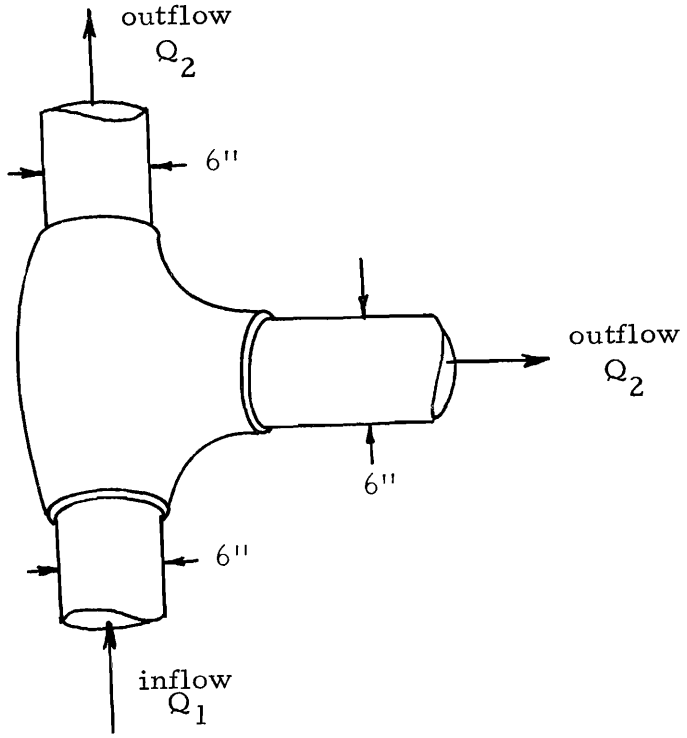

Fig. 3. Operation of 6 x 6 x 6-inch RING-TITE filament wound tee separating the inflow into two branches of outflow.

7. Determination of the head losses due to a 6x6x6-inch RING-TITE filament-wound tee operating to combine flows from one of the "straight through" branches and the 90° branch into a single discharge through the other "straight through" branch as illustrated in Fig. 4.

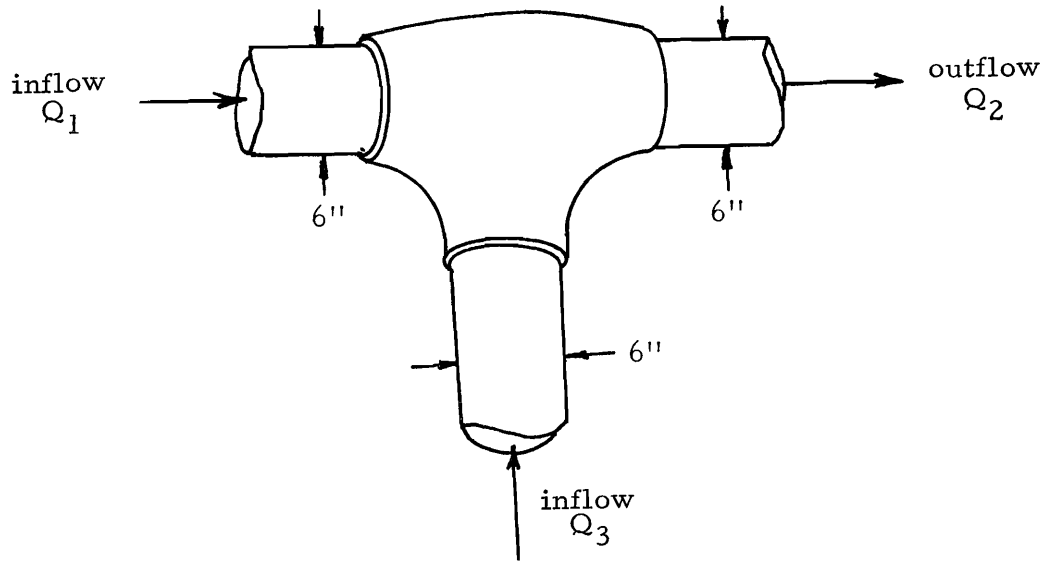

Fig. 4. Operation of the 6 x 6 x 6-inch RING-TITE filament wound tee acting to combine two inflows into a single outflow.

The above determinations were based on flow rates from 150 gpm (in the 6-inch pipes) to as large a flow rate as could be achieved from the UWRL water supply from the Logan River which had approximately 27 feet of head available between the laboratory floor and the reservoir, or to 1500 gpm when this flow rate could be achieved.

TEST SET-UPS

The tests needed to provide data for accomplishing the objectives outlined previously were conducted on the hydraulic floor area in the Utah Water Research Laboratory. The water supply used was Logan River water, which is diverted at the "First Dam" through a 48-inch pipe to the laboratory, where it is directed throughout the laboratory by means of a network of 18, 24, and 36-inch pipes. The supply was taken from the 36-inch pipe of this network. The 27 feet of available head turned out to be inadequate to achieve a maximum desired flow rate of 1500 gpm through the pipes in all tests. There were no booster pumps available in the present laboratory distribution network appropriate to use in these tests to obtain the maximum desired flow rate for all tests.

The data required to achieve the items listed under "objectives" required five separate lay-outs of the pipes and fittings. These arrangements of pipes, fittings, piezometer boards and meters have been numbered as lay-out No. 1 through lay-out No. 5 for subsequent reference. Schematic diagrams of these five separate lay-outs are given in Figs. 5 through 9 respectively. Photographs of lay-out No. 1 are contained on Fig. 10.

Lay-out No. 1 (Fig. 5) was used to collect data to simultaneously determine the frictional loss in 6-inch PERMASTRAN® pipe and the head loss due to the 6-inch RING-TITE filament-wound 90° elbow (objective 3). In this lay-out three points were selected for pressure taps in the three sections of 20-ft long PVC pipe upstream from the elbow. Seven 20-ft sections of 6-inch PERMASTRAN® pipe were placed downstream (with the bell in the downstream direction), with pressure taps placed 1.5 feet from the ends of the pipe sections. The exact position of the pressure taps is given in the table contained on Fig. 5. The pressure taps were constructed by tapping a 3/16-inch hole through

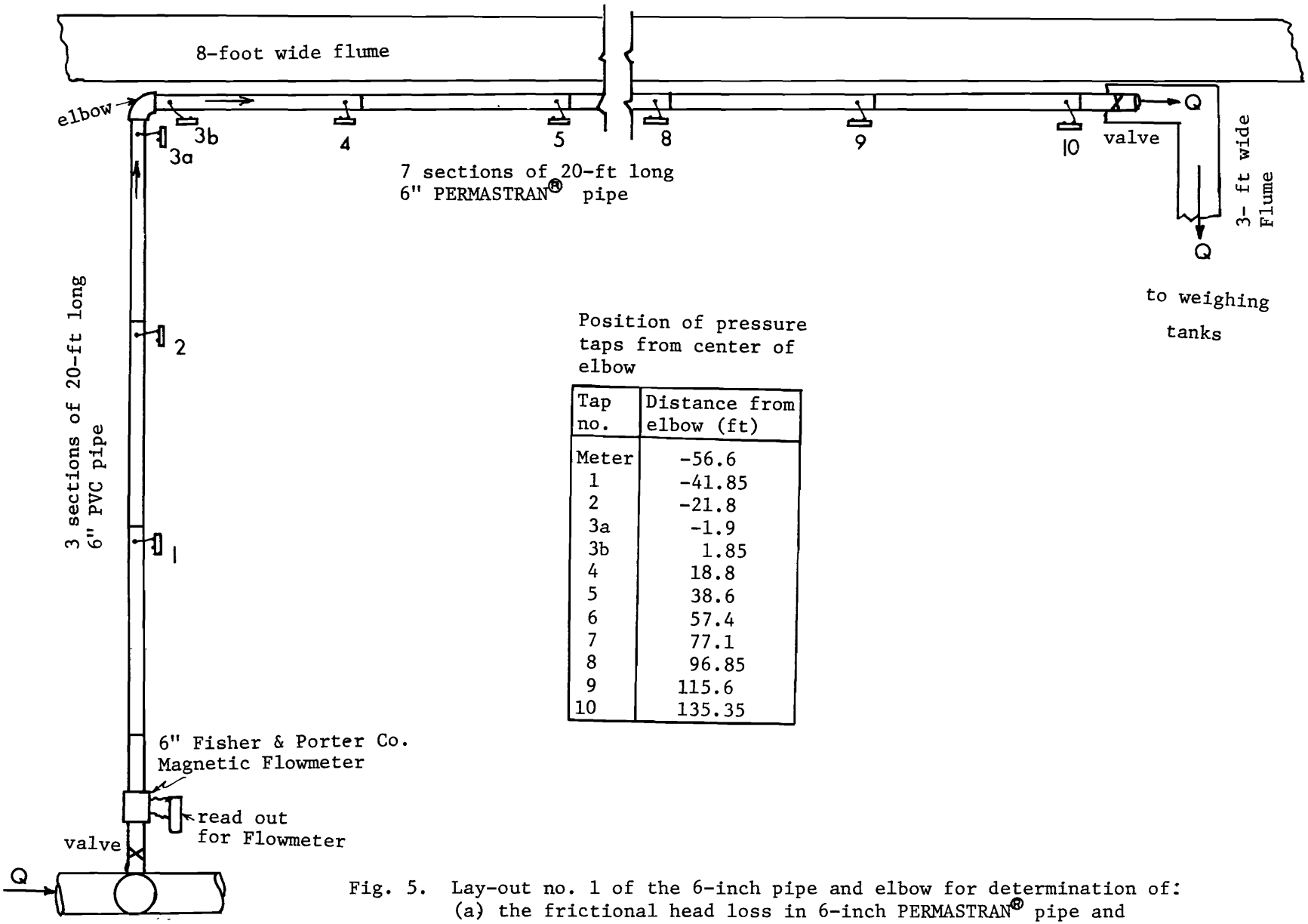

Position of pressure taps from center of elbow

Tap no.	Distance from elbow (ft)
Meter	-56.6
1	-41.85
2	-21.8
3a	-1.9
3b	1.85
4	18.8
5	38.6
6	57.4
7	77.1
8	96.85
9	115.6
10	135.35

Fig. 5. Lay-out no. 1 of the 6-inch pipe and elbow for determination of:
(a) the frictional head loss in 6-inch PERMASTRAN® pipe and
(b) the losses due to a 6-inch RING-TITE Filament wound 90° elbow.

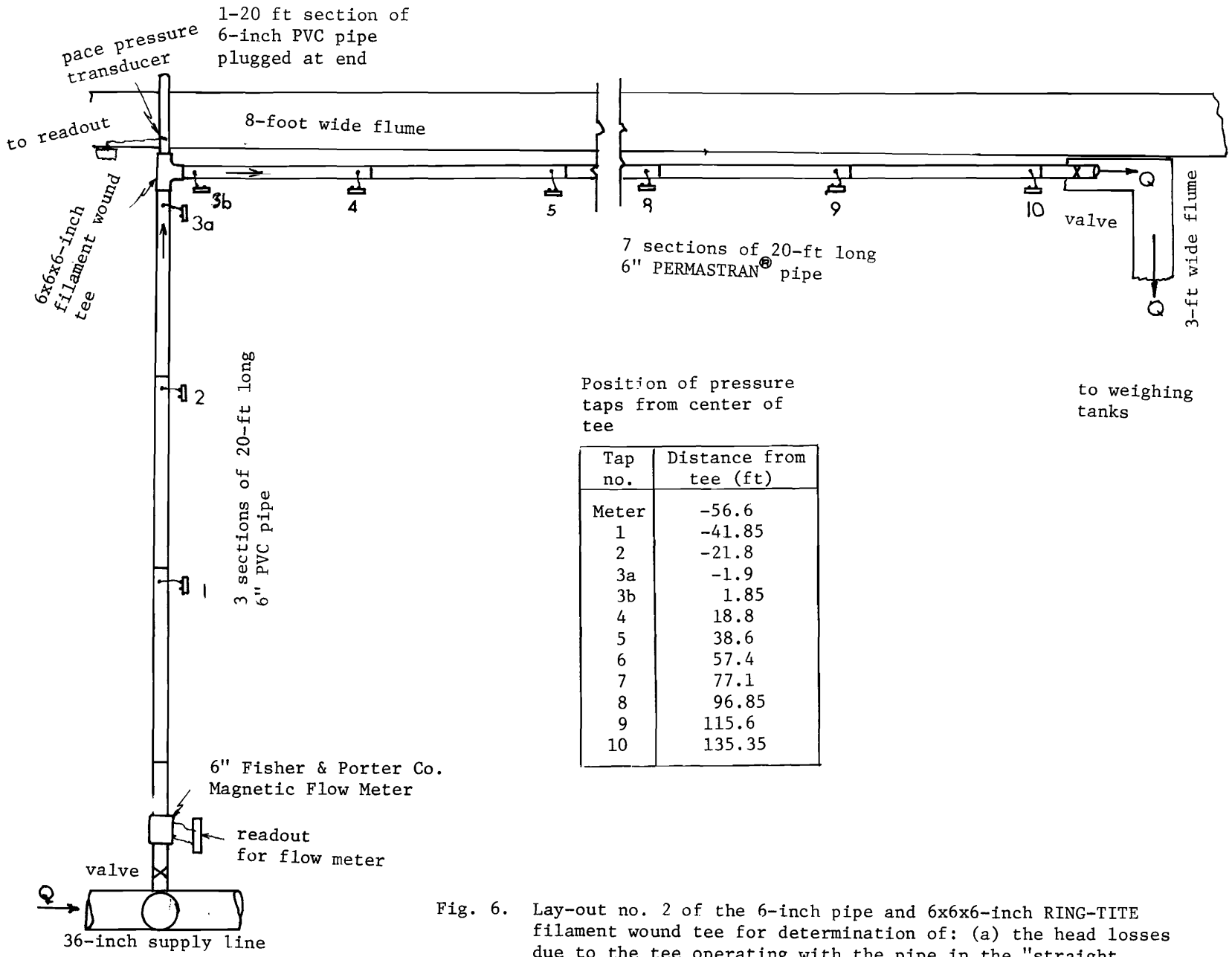

Position of pressure taps from center of tee

Tap no.	Distance from tee (ft)
Meter	-56.6
1	-41.85
2	-21.8
3a	-1.9
3b	1.85
4	18.8
5	38.6
6	57.4
7	77.1
8	96.85
9	115.6
10	135.35

to weighing tanks

Fig. 6. Lay-out no. 2 of the 6-inch pipe and 6x6x6-inch RING-TITE filament wound tee for determination of: (a) the head losses due to the tee operating with the pipe in the "straight through" direction of the inflow plugged, and (b) verification of the frictional head losses in 6-inch PERMASTRAN® pipe.

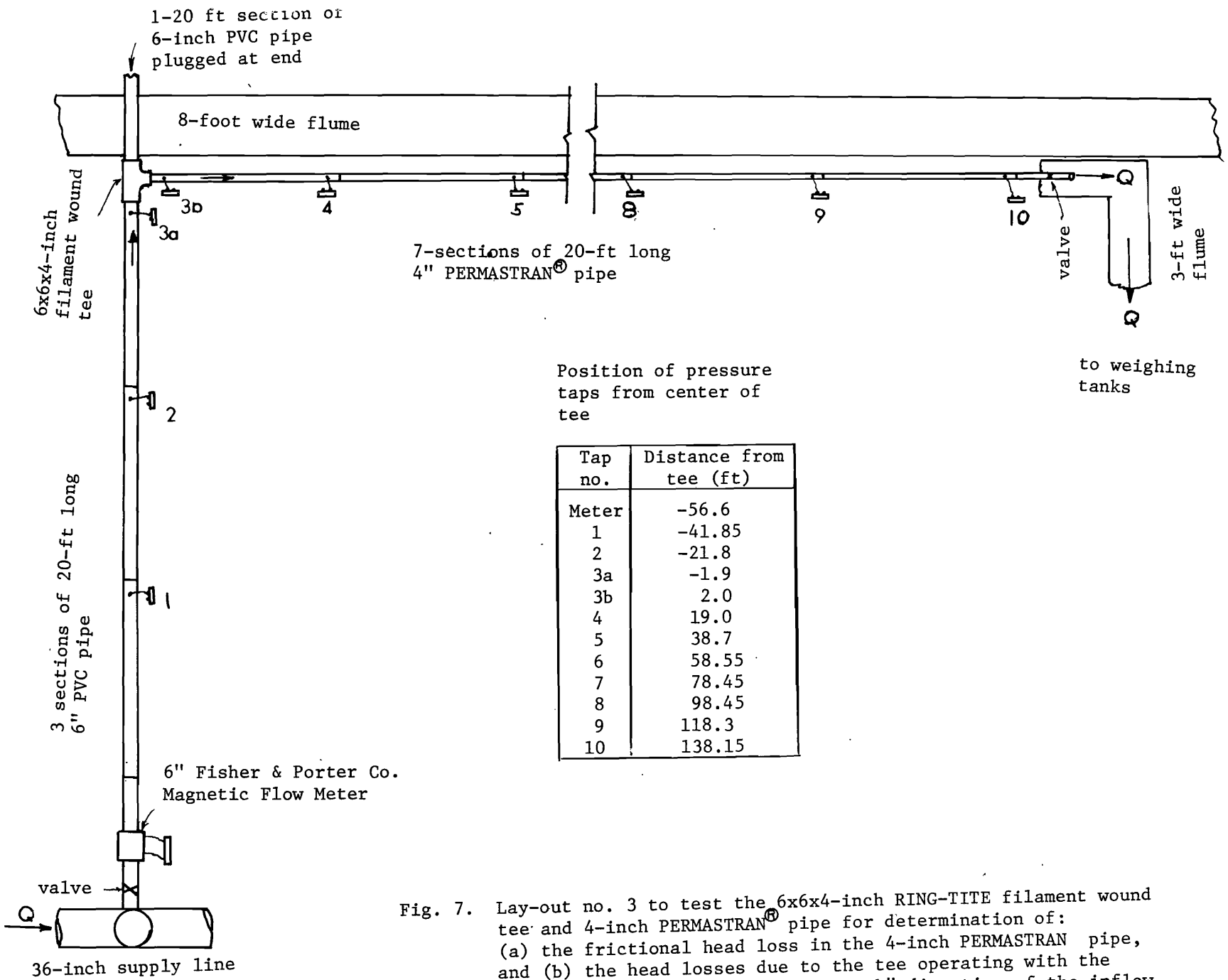

Position of pressure taps from center of tee

Tap no.	Distance from tee (ft)
Meter	-56.6
1	-41.85
2	-21.8
3a	-1.9
3b	2.0
4	19.0
5	38.7
6	58.55
7	78.45
8	98.45
9	118.3
10	138.15

Fig. 7. Lay-out no. 3 to test the 6x6x4-inch RING-TITE filament wound tee and 4-inch PERMASTRAN® pipe for determination of: (a) the frictional head loss in the 4-inch PERMASTRAN pipe, and (b) the head losses due to the tee operating with the 6-inch pipe in the "straight through" direction of the inflow plugged.

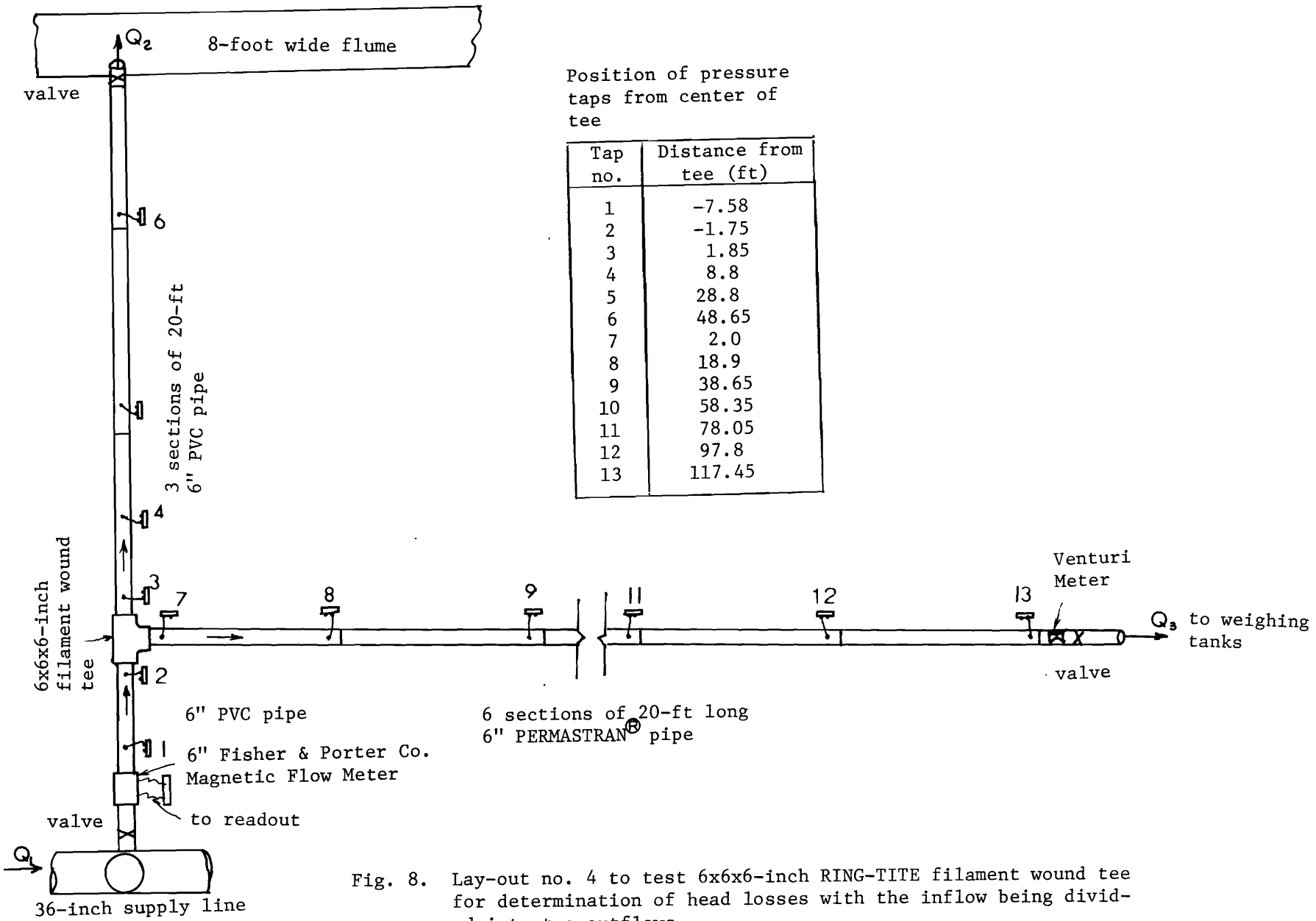

Position of pressure taps from center of tee

Tap no.	Distance from tee (ft)
1	-7.58
2	-1.75
3	1.85
4	8.8
5	28.8
6	48.65
7	2.0
8	18.9
9	38.65
10	58.35
11	78.05
12	97.8
13	117.45

Fig. 8. Lay-out no. 4 to test 6x6x6-inch RING-TITE filament wound tee for determination of head losses with the inflow being divided into two outflows.

Position of pressure taps from center of tee

Tap no.	Distance from tee (ft)
1	-7.58
2	-1.75
3	
4	
5	2.0
6	18.9
7	38.65
8	58.35
9	78.05
10	97.8
11	117.45

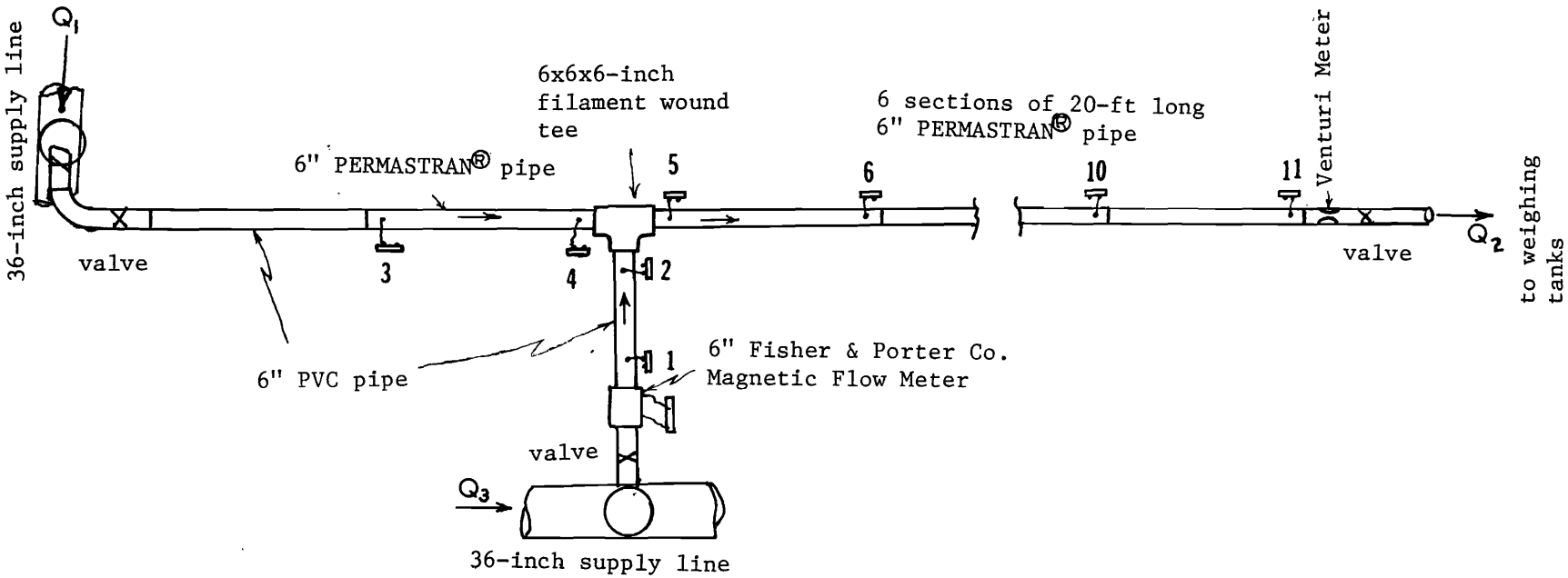

Fig. 9. Lay-out no. 5 to test 6x6x6-inch RING-TITE filament wound tee for determination of head losses with two inflows being combined into one outflow.

looking upstream from elbow at test pipe line

looking downstream from elbow at test pipe line

Fig. 10. Photographs showing the experimental lay-out No. 1 at the UWRL looking upstream and downstream from the elbow.

the pipe wall and screwing a grease fitting into this tapped hole after the ball and spring from within the grease fitting were removed. A plastic tube directed the water from the pressure tap to a 4-foot long manometer board containing mercury as the manometer fluid. These pressure taps were carefully drilled to prevent distortion of the pipe wall in their immediate vicinity. After screwing the grease fitting in place, any burrs left by the installation process were removed by hand sanding with a very fine wet-dry paper. The pipe was installed in place so that the pressure taps were located on the top of the pipe, when one tap was located at a section and on top and the two sides where three taps were located at a section.

After taking data for the first series of tests, more scatter existed in the data than seemed desirable for establishing the position of the energy line. Consequently to ascertain if this scatter might be due to not measuring a representative pressure at all sections two additional taps on each side of the pipe were installed at section Nos. 3a, 3b, 5 and 10 on Fig. 5. Subsequent measurements at these sections gave identical readings for all three taps, so, consequently, tables giving this data show only one reading at a given section. The conclusion was that representative pressures were being obtained.

The piezometric heads at each of the pressure taps were determined from the reading of the manometer boards. To eliminate any variation in the elevation of the laboratory floor on which the tests were conducted, a datum was established on each manometer board after it was put in position on the floor. This datum was established with an engineers level set-up near the pipe elbow. The engineers level was checked immediately prior to establishing this datum to ensure that it was in proper adjustment. This same procedure of establishing a datum on the manometer boards was followed for each of the lay-outs.

Using this datum as a reference the piezometric heads (sum of elevation and pressure heads) at each section where a pressure tap

exists were determined (in inches of water) from the equations (see Fig. 11 for notation used in Eqs. 8 and 9),

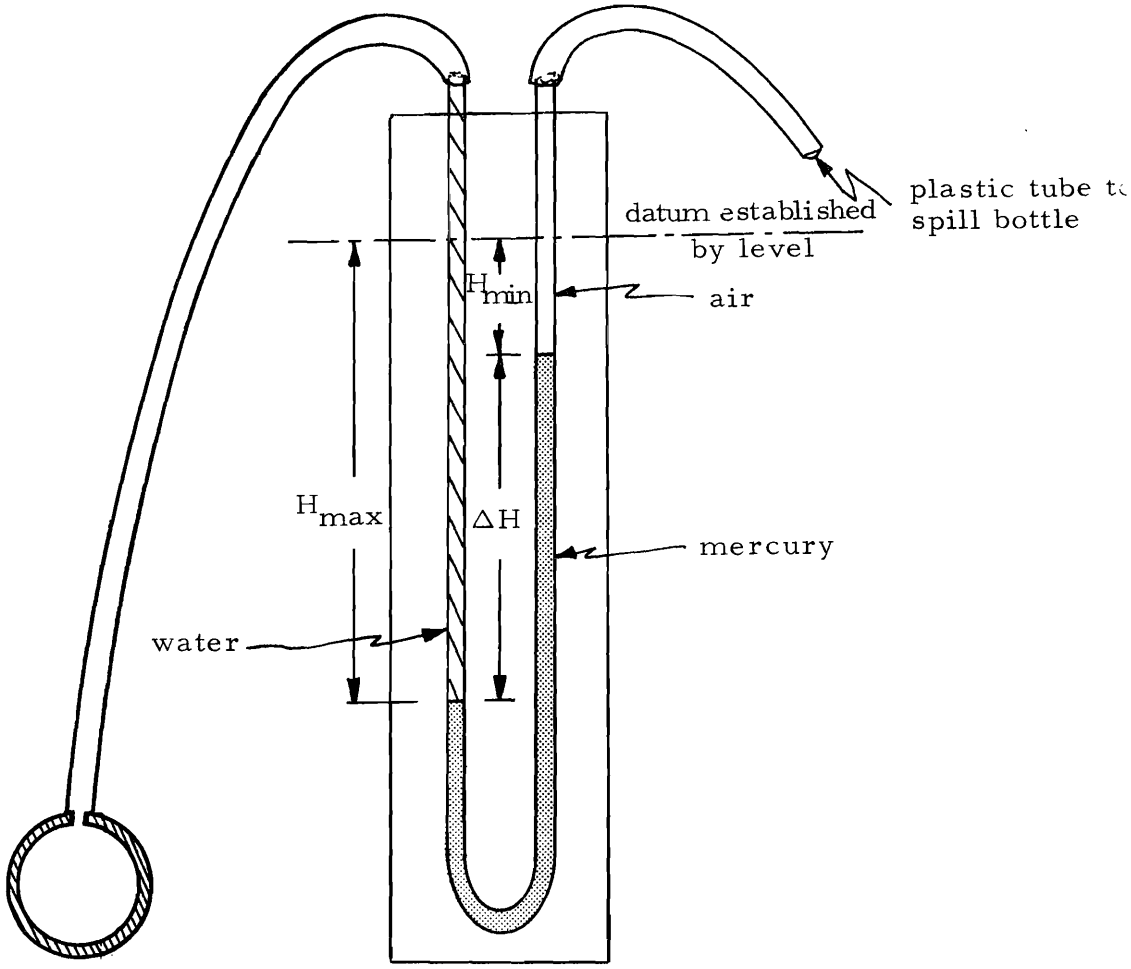

Fig. 11. Sketch of manometer board.

$$H_p = 13.55\Delta H - H_{max} \quad . \quad . \quad . \quad . \quad . \quad . \quad . \quad . \quad . \quad . \quad (8)$$

or

$$H_p = 12.55\Delta H - H_{min} \quad . \quad . \quad . \quad . \quad . \quad . \quad . \quad . \quad . \quad . \quad (9)$$

depending upon whether H_{max} or H_{min} was recorded, in which H_p is the piezometric head above the datum established by the level (Δz above the pipe center), 13.55 equals the specific gravity of mercury,

ΔH is the difference in height of the mercury columns in inches, and H_{max} and H_{min} are the distances in inches below the data of the lower and upper columns of mercury, respectively.

The head in feet of water at any section can be obtained by dividing H_p from Eq. 8 or 9 by 12, and this in turn can be converted to pressure in psi above the datum by multiplying by .4333. The position of the energy line can be obtained by adding the velocity head to the piezometric head. The head losses are the drops in the position of the energy line.

Data from four series of tests were obtained from lay-out No. 1. These are referred to as test series Nos. 1, 2, 3 and 4 in subsequent tables and references.

Lay-out No. 2 is almost identical to No. 1 with the exception that the elbow is replaced by the 6 x 6 x 6-inch RING-TITE filament wound tee, and a length of 20-ft PVC pipe was placed in the branch of the tee extending "straight through" from inlet branch. At its end this PVC pipe was capped so the entire flow was forced to turn through 90^{o} within the tee. Thus the tee acted as a 90^{o} elbow. Data referred to as test series 5 were obtained from lay-out No. 2, and these data were used for determining the loss coefficient for the 6 x 6 x 6-inch tee operating as shown in Fig. 1 and also to verify the frictional losses in the 6-inch PERMASTRAN® pipe which were determined from the data series of lay-out No. 1.

In lay-out No. 3 (Fig. 7) the 6 x 6 x 4-inch RING-TITE filament wound tee was installed in the position of the 6 x 6 x 6-inch tee in lay-out No. 2 and the downstream line was replaced by 4-inch pipe. The first four 20-ft long sections of this downstream 4-inch line were PERMASTRAN® pipe, and the last three sections were PVC pipe, each 20 feet long. Ideally only PERMASTRAN® pipe would have been used. The only hydraulic difference between these two pipes, however, is a slight difference in internal diameter, since the PERMASTRAN®

pipe has a polyvinylchloride liner, the material used in construction of PVC pipe. Data for test series No. 6 were obtained from lay-out No. 3. These data were used to determine the loss coefficient for the 6x6x4-inch tee operating as shown in Fig. 2, and also the frictional head loss in the 4-inch PERMASTRAN® pipe.

Lay-out No. 4 (Fig. 8) was designed to divide the flow from the inlet branch into the two outlet branches of the 6x6x6-inch tee. For this lay-out the tee was placed at a distance 13 feet from the 6-inch magnetic flow meter, and a 3-inch throat diameter Venturi meter, followed by a valve, was installed at the end of the downstream line in the 90° direction from the inflow, and the other downstream line (also fitted with a valve) discharged into the large 8-ft wide flume. By adjusting the valves on the two outflow lines and reading both the magnetic and Venturi meters the flow rates through each outlet branch could be determined or set as desired. Many of the tests split the inflow equally in the two outflow branches. Data referred to as test series No. 7 were obtained from lay-out No. 4. These data were used to determine the minor losses and loss coefficients for the 6x6x6-inch tee operating as shown in Fig. 3.

Lay-out No. 5 (Fig. 9) was used to obtain data for test series No. 8. In this lay-out water was taken from two separate points of the 36-inch laboratory supply line and directed into two sides of the 6x6x6-inch tee. These flows were combined in the tee and discharged through one of the "straight through" branches. To measure the flow in the two inlets, the flow through one of the inlet branches was metered with the magnetic flow meter, and the combined flow metered with the enturi meter until its capacity was exceeded, and thereafter the total flow rate was determined by directing the water into the weighing tanks. Meters were calibrated in place of the weighing tank for all lay-outs. Their use aided in establishing a predetermined flow rate in each line, when both meters could be used.

EXPERIMENTAL PROCEDURE

After having the pipes, etc. installed according to lay-out No. 1 the magnetic flow meter was calibrated in place. This calibration was accomplished by directing the outflow water into the two automatic recording weighing tanks in the Utah Water Research Laboratory. The calibration included eight different flow rates from just under 150 gpm to the maximum flow (1, 280 gpm) that was possible with the head available with the river water supply. This calibration curve was plotted on the circular read-out of the magnetic flow meter so that for all tests it was possible to establish a flow rate of predetermined increments of 100 gpm.

To ascertain how accurately the flow rates could actually be set by adjusting the dial to an increment of 100 gpm on the calibration curve, the flows from the first and second series of tests were directed into the weighing tanks during the tests and the actual flow rates compared with those that were to have been established. The largest difference between these two flow rates was 4 gpm. Because of this close agreement it was evident that adjusting the valve until the dial of the flow meter was on a predetermined flow rate value was satisfactory and it was not necessary to actually weigh the water for each test. Therefore, after collecting the data from the pressure taps from what is referred to as test series No. 2, the outflow water was no longer directed into the weighing tanks (excepted when the capacity of the Venturi meter was exceeded in a test).

For lay-out Nos. 4 and 5 which required two flow meters to insure equal flows in the branches of the tee, it was necessary to calibrate the second meter. A 3-inch throat diameter Venturi meter was used for this second meter. It was also calibrated in place following the previously described procedure of directing the outflow from this line

into the weighing tanks. As with the magnetic meter after calibration of the Venturi meter, some predetermined flow rates were checked by weighing. Less than 4 gpm existed between the established and actual flow rates.

The water supply was at a constant head at the "First Dam" for all practical purposes during any test because the small flow rates withdrawn for these tests were insignificant in comparison to the river flow, which goes over the dam spillway. Despite this fact the ability of the system to maintain established flow rates over extended periods of time was checked. This check was conveniently accomplished by regularly checking the setting on the meter (or meters) to see if it remained at the same setting as at the beginning of the test. All of these checks showed no variation in the established flow rates even during a time when another experiment being conducted simultaneously was using up to 10 cfs from the same river supply.

For each test both H_{min} (or H_{max}) and ΔH (see Fig. 11) were recorded from each manometer attached to a pressure tap. This recorded data was subsequently punched onto data cards and processed by a digital computer. Tables 1 and 2 give the results from the initial processing of this data. In these tables the piezometric heads are given as computed by Eq. 8 or 9 and the total energy heads are given as the piezometric head plus the velocity head. Test series 1 through 6 are contained in Table 1, with series 1 through 4 using lay-out 1, series 5 using lay-out 2, and series 6 using lay-out 3. The numbering of the sections in these 6 series of tests are as noted on Figs. 5 through 9, with numbers 1, 2, and 3a upstream from the elbow or tee and sections 3b through 10 downstream of the elbow and tee for the first 3 lay-outs. A slightly different numbering system was used for the last two lay-outs.

ANALYSES OF TEST DATA

Reliability of Data

To fully understand the analyses of the data and interpret the results from these analyses properly the, reader should have an understanding of the accuracy of the data. The piezometric head and total energy head data recorded in Tables 1 and 2 are given to one-tenth of an inch. This precision is beyond the accuracy with which the data could be recorded. As is characteristic of turbulent flows in general, continual small pressure fluctuations were noted particularly during the higher flow rates. These fluctuations were particularly large when the tees were in the line with the extension of the inlet line plugged, i.e. test series 5 and 6. These large fluctuations are described in greater detail later. These pressure fluctuations caused the positions of the mercury columns in the piezometers to change continually. For the lower flow rates these fluctuations were hardly noticeable, but at the higher flow rates the movement of the mercury columns was quite noticeable. These fluctuations made it difficult to measure values for H_{min} and ΔH from the manometer with greater precision than the nearest one-tenth of an inch, even though in most cases an estimate to the nearest one-hundredth of an inch was actually recorded. However, since the specific gravity of mercury is 13.55 the computed piezometric head will in general be only one-thirteenth as precise as the recorded data. Consequently, the data for piezometric head, and total energy head which are given in Tables 1 and 2 can be considered correct only to the nearest inch of water.

Record of Pressure Fluctuations

When the 6 x 6 x 6-inch tee was installed as in lay-out No. 2 with the extension of the inlet pipe closed the continual bouncing of the mercury

Table 1. Piezometric and total energy head data computed from the laboratory manometer data obtained from the pressure taps for test series 1 through 6.

TEST SERIES	FLOW RATE (GPM)	SECTION OF PRESSURE TAP																					
		1		2		3A		3B		4		5		6		7		8		9		10	
		H_p	E	H_p	E	H_p	F	H_p	E	H_p	F	H_p	E	H_p	E	H_p	E	H_p	E	H_p	E	H_p	E
1	150	101.7	102.2	101.9	102.4	104.5	105.0			101.4	101.9	99.9	100.3	103.0	103.5	104.7	105.2	99.2	99.7	100.1	100.6	100.8	101.3
	200	114.8	115.7	112.5	113.4	113.7	114.6			111.9	112.7	110.3	111.1	110.8	111.6	111.2	112.0	109.7	110.5	109.2	110.0	107.2	108.0
	300	278.0	280.0	276.9	278.9	276.8	278.8			273.8	275.6	272.0	273.9	272.4	274.3	270.3	272.2	268.9	270.7	266.9	268.7	263.8	265.6
	400	101.7	105.4	100.7	104.3	100.6	104.2			95.0	98.2	92.1	95.3	91.3	94.6	90.3	93.6	86.2	89.4	83.1	86.4	79.8	83.0
	500	176.2	181.8	172.4	178.1	171.1	176.7			162.8	167.9	158.6	163.7	156.4	161.5	154.1	159.2	150.1	155.2	145.7	150.8	143.8	148.8
	600	159.2	167.3	155.4	163.5	151.6	159.7			140.6	147.9	136.3	143.7	134.2	141.5	130.7	138.1	124.1	131.4	119.7	127.0	112.4	119.8
	731	181.4	193.5	175.0	187.1	169.7	181.8			155.0	165.9	148.1	159.0	139.5	150.4	137.3	148.2	127.9	138.8	123.5	134.4	113.8	124.7
2	150	297.5	298.0	298.3	298.9	297.6	298.1			298.6	299.1	298.1	298.6	298.4	298.9	297.8	298.2	297.6	298.0	297.0	297.5	291.4	291.8
	300	43.0	45.0	41.3	43.3	38.1	40.1			37.3	39.2	34.6	36.5	33.9	35.7	38.2	40.1	32.7	34.6	29.8	31.6	28.8	30.6
	600	59.9	68.0	55.9	64.0	49.8	57.9			42.8	50.1	37.2	44.6	32.5	39.9	31.7	39.0	24.9	32.2	20.6	27.9	15.8	23.1
	750	104.2	117.0	100.3	113.0	88.9	101.6			77.9	89.4	72.4	83.9	63.8	75.3	59.0	70.5	52.2	63.7	44.1	55.5	37.9	49.4
	900	164.4	182.7	155.1	173.4	142.4	160.7			124.9	141.4	116.8	133.3	105.6	122.1	98.2	114.7	88.8	105.3	79.3	95.8	70.5	87.0
	1200	216.6	249.1	198.1	230.6	181.5	214.1			151.1	180.5	135.1	164.4	115.9	145.3	103.4	132.7	88.8	118.1	74.1	103.5	57.5	86.8
	1300	202.2	240.3	181.2	219.4	160.2	198.9			127.6	162.1	107.7	142.1	87.3	121.7	73.4	107.8	54.9	89.3	37.6	72.0	21.0	55.4
3	1200	166.9	199.4	151.1	183.7	133.2	165.7			104.1	133.5	86.8	116.2	69.1	98.4	59.0	88.3	41.8	71.1	28.4	57.7	11.8	41.1
	900	89.8	108.1	79.4	97.7	69.3	87.6			50.6	67.1	41.1	57.6	30.0	46.5	23.8	40.3	13.1	29.6	3.7	20.2	-6.5	10.0
	750	197.0	209.7	190.3	203.0	180.3	193.0			169.4	180.9	162.4	173.9	153.8	165.3	147.8	159.2	139.6	151.1	134.0	145.4	128.0	139.4
	600	117.3	125.4	111.8	119.9	105.8	114.0			97.6	104.9	92.1	99.4	86.1	93.4	85.1	92.5	79.6	86.9	75.4	82.7	70.6	77.9
	1300	203.5	241.7	182.2	220.4	162.0	200.2			127.6	162.1	109.0	143.4	87.3	121.7	73.4	107.8	56.2	90.6	38.9	73.3	19.6	54.0
4	200	63.7	64.6	63.8	64.8	60.1	61.0	60.5	61.3	58.2	59.0	58.7	59.5	58.0	58.8	59.0	59.8	59.4	60.2	56.1	56.0	55.5	56.4
	400	79.3	82.9	77.6	81.2	73.2	76.8	71.6	74.9	69.9	73.2	67.2	70.4	63.8	67.1	62.9	66.1	62.1	65.3	59.1	62.3	56.8	60.1
	500	138.0	143.7	133.7	139.3	129.9	135.6	125.0	130.1	123.6	128.7	120.0	125.1	116.0	121.1	113.7	118.8	110.3	115.4	106.6	111.7	101.9	107.0
	600	73.4	81.5	69.1	77.3	61.4	69.6	57.2	64.5	54.3	61.6	48.2	55.5	43.6	51.0	40.1	47.4	37.3	44.6	31.0	38.4	25.5	32.9
	750	130.2	142.9	121.9	134.6	117.5	130.3	104.9	116.3	101.3	112.7	93.2	104.7	85.4	96.8	81.1	92.6	71.8	83.2	66.8	78.2	59.5	70.9
	900	190.9	209.2	180.8	199.1	168.4	186.7	159.0	175.5	152.9	169.4	142.1	158.6	131.6	148.1	125.5	142.0	113.5	130.0	105.4	121.9	95.4	111.9
	1200	170.8	203.3	152.1	184.6	134.5	167.0	115.3	144.6	104.6	133.9	89.3	118.6	69.1	98.4	57.7	87.0	43.1	72.4	20.4	49.7	10.5	39.9
5	150	54.7	55.2	58.5	59.0	53.5	54.1	53.3	53.8	53.0	53.5	52.8	53.3	52.1	52.6	51.8	52.3	51.6	52.0	49.9	50.4	49.6	50.1
	300	250.5	252.5	250.3	252.3	248.0	250.1	243.8	245.7	242.3	244.1	241.3	243.1	241.1	243.0	239.6	241.4	238.8	240.6	235.5	237.3	235.6	237.5
	400	137.0	140.6	136.7	140.3	130.6	134.2	125.1	128.3	123.5	126.7	121.9	125.2	119.9	123.2	119.5	122.8	116.1	119.4	113.1	116.3	109.0	112.3
	500	106.9	112.6	105.4	111.1	96.3	101.0	89.8	94.9	86.9	92.0	83.4	88.5	79.6	84.6	75.9	81.0	73.0	78.1	68.1	73.2	65.3	70.4
	600	153.8	162.0	150.4	158.5	144.9	153.0	134.9	142.2	132.7	140.0	127.1	134.5	121.9	129.2	117.1	124.4	113.5	120.9	107.9	115.2	102.5	109.9
	750	152.0	164.7	141.3	154.0	133.9	146.5	119.9	131.3	113.0	124.5	104.3	115.7	97.8	109.3	92.9	104.3	86.2	97.6	79.2	90.7	71.8	83.2
	900	197.0	215.3	186.4	204.7	178.8	197.1	151.9	168.3	148.3	164.8	134.2	150.7	123.2	139.7	117.6	134.1	108.3	124.8	97.5	114.0	88.1	104.6
	1050	195.6	220.6	181.2	206.1	165.8	190.7	134.2	156.7	122.9	145.3	112.8	135.3	100.4	122.8	88.9	111.4	78.3	100.8	63.4	85.9	49.6	72.0
	1200	191.8	224.3	179.8	212.4	159.3	191.8	126.3	155.7	110.5	139.8	95.8	125.1	75.4	104.8	58.3	87.7	45.0	74.4	30.4	59.7	13.1	42.4
6	50	116.0	116.1	119.8	119.8	115.6	115.7	115.2	115.5	115.6	115.9	112.7	113.0	112.1	112.3	112.4	112.7	112.2	112.5	109.1	109.4	109.0	109.3
	100	75.5	75.7	73.7	73.9	74.5	74.8	71.5	72.5	69.9	70.9	68.4	69.3	69.1	70.0	68.7	69.8	66.5	67.6	64.1	65.2	62.1	63.1
	200	86.6	87.5	89.9	90.8	86.2	87.1	76.7	80.6	71.3	75.2	68.4	72.2	62.6	66.5	60.2	64.5	52.2	56.5	46.5	50.8	41.8	46.1
	300	218.5	220.5	215.1	217.1	213.4	215.5	194.9	203.6	187.4	196.1	174.7	183.4	165.5	174.3	158.1	167.7	144.9	154.5	135.1	144.7	127.3	136.9
	400	167.8	171.5	145.3	148.9	121.8	125.5	103.0	119.5	116.9	132.4	101.0	116.5	80.8	96.3	67.4	84.5	48.3	65.4	31.6	48.6	13.1	30.2
	500	253.1	258.7	251.6	257.3	246.1	251.8	187.6	211.3	168.8	193.1	167.5	191.7	161.9	186.7	122.4	149.1	76.3	103.0	48.5	75.2	19.0	45.7
	577	290.2	297.8	287.4	295.0	283.3	290.9	208.6	240.9	173.6	205.9	161.0	193.3	123.8	156.1	104.0	139.5	68.5	104.1	34.2	69.7	17.0	52.6

Table 2. Piezometric and total energy head data computed from the laboratory manometer data obtained from the pressure taps for test series 7 and 8.

TEST	FLOW RATE			SECTION OF PRESSURE TAP																	
SER	(GPM)			1		2		3		4		5		6		7		8		9	
IES	Q_1	Q_2	Q_3	H_p	E	H_p	E	H_p	E	H_p	E	H_p	E	H_p	E	H_p	E	H_p	E	H_p	E
7	200	100	100	118.5	119.4	117.5	118.4	117.5	117.7	117.3	117.6	116.7	116.9	116.4	116.6	116.8	117.0	117.6	117.8	115.0	115.2
	400	200	200	152.4	156.0	150.1	153.8	150.1	151.1	151.3	152.2	150.6	151.5	149.7	150.6	147.5	148.4	147.7	148.5	147.0	147.8
	600	300	300	209.8	217.9	208.8	217.0	212.8	214.8	210.0	212.1	208.6	210.7	215.0	217.0	204.3	206.1	202.5	204.3	200.9	202.3
	800	400	400	115.2	129.6	113.5	128.0	118.2	121.8	118.6	122.2	116.0	119.6	113.1	116.7	107.7	110.9	105.3	108.5	100.0	103.3
	1000	500	500	95.6	118.2	92.6	115.2	102.5	108.1	101.0	106.6	97.1	102.7	96.9	102.5	80.9	86.0	77.2	82.3	72.7	77.8
	1200	1000	200	176.5	209.1	179.3	211.8	179.3	201.8	164.3	186.9	149.9	172.4	137.3	159.9	163.8	164.6	163.4	164.2	162.7	163.5
	1200	800	400	170.1	202.6	167.1	199.6	177.5	192.0	174.7	189.2	164.3	178.7	158.7	173.2	157.9	161.1	154.8	158.1	153.5	156.7
	1200	600	600	173.3	205.8	165.8	198.3	182.7	190.9	181.3	189.5	173.3	181.5	171.8	179.9	153.9	161.2	146.3	153.7	140.4	147.8
	1500	765	735	202.6	253.5	194.6	245.4	221.6	234.8	218.9	232.1	210.9	224.2	202.9	216.1	169.7	180.7	164.6	175.6	155.9	166.9

FLOWRATES (GPM)			SECTION OF PRESSURE TAP							
			10		11		12		13	
Q_1	Q_2	Q_3	H_p	E	H_p	E	H_p	E	H_p	E
200	100	100	115.0	115.2	115.3	115.5	115.3	115.5	113.4	113.6
400	200	200	145.7	146.5	145.2	146.0	144.0	144.8	142.8	143.6
600	300	300	198.4	200.3	200.0	201.8	196.2	198.0	194.2	196.0
800	400	400	97.4	100.7	95.7	99.0	94.4	97.6	91.1	94.4
1000	500	500	70.1	75.2	65.7	70.8	63.1	68.2	59.8	64.9
1200	1000	200	160.0	160.8	160.8	161.7	159.6	160.4	159.0	159.8
1200	800	400	150.9	154.1	149.1	152.4	145.9	149.2	144.0	147.3
1200	600	600	132.3	139.6	126.8	134.1	123.1	130.4	125.6	132.9
1500	765	735	150.9	161.9	146.5	157.5	138.8	149.8	128.9	139.9

TEST	FLOW RATE			SECTION OF PRESSURE TAP																	
SER	(GPM)			1		2		3		4		5		6		7		8		9	
IES	Q_2	Q_1	Q_3	H_p	E	H_p	E	H_p	E	H_p	E	H_p	E	H_p	E	H_p	E	H_p	E	H_p	E
8	200	100	100	249.6	249.9	249.3	249.6	251.9	252.2	248.6	248.8	246.7	247.5	246.9	247.7	245.9	246.7	244.3	245.6	245.0	245.9
	400	200	200	197.4	198.3	195.1	196.0	198.4	199.2	195.9	196.7	191.9	195.2	190.1	193.4	187.2	190.5	185.4	188.6	184.3	187.6
	600	300	300	236.6	238.6	235.6	237.6	240.2	242.0	236.3	238.1	227.8	235.1	223.4	230.7	219.1	226.4	213.9	220.7	211.1	218.4
	800	400	400	267.2	270.8	265.0	268.6	269.5	272.8	265.6	268.8	251.9	265.0	244.9	258.0	237.4	250.4	227.7	240.8	222.8	235.9
	780	380	400	267.2	270.8	265.0	268.6	269.5	272.5	265.8	268.5	251.9	264.3	244.9	257.3	237.4	249.8	227.7	240.1	222.8	235.2
	1070	570	500	153.7	159.4	153.3	159.0	160.3	166.9	153.3	159.9	127.9	151.2	115.0	138.3	100.5	123.8	83.7	107.1	77.1	100.4
	1210	610	600	194.8	203.0	193.8	202.0	201.4	209.0	194.9	202.1	158.1	187.9	147.0	176.8	131.0	160.8	102.8	132.7	96.1	125.9
	1485	735	750	280.9	293.7	278.0	290.7	290.3	301.3	281.4	292.4	231.1	276.0	206.5	251.4	183.9	228.8	152.8	197.7	135.8	180.7
	600	400	200	265.7	266.6	259.1	260.0	263.7	267.0	259.7	262.9	251.3	258.6	247.6	254.9	243.3	250.6	237.5	244.9	234.3	241.6
	600	200	400	184.4	188.0	182.7	186.3	186.8	187.6	182.8	183.6	174.9	182.2	169.8	177.2	165.6	173.0	159.9	167.2	157.4	164.7
	1065	465	600	149.2	157.3	146.8	154.9	153.2	157.6	125.9	130.3	121.3	144.4	108.7	131.8	95.8	118.9	77.3	100.9	69.3	92.4
	1070	670	400	143.0	146.6	142.2	145.8	148.0	157.1	137.8	147.0	118.7	142.0	106.8	130.1	94.6	117.9	77.2	100.5	68.0	91.3
	1430	430	1000	263.9	286.5	257.2	279.7	268.0	271.8	264.4	268.2	214.0	255.7	192.3	233.9	170.9	212.5	142.4	184.0	126.0	167.6
	1450	950	500	260.1	265.7	255.8	261.5	268.0	286.4	255.3	273.6	215.4	258.2	194.3	237.1	173.5	216.3	143.7	186.5	128.0	170.8

FLOWRATES (GPM)			SECTION OF PRESSURE TAP			
			10		11	
Q_2	Q_1	Q_3	H_p	E	H_p	E
200	100	100	244.4	245.2	243.2	244.0
400	200	200	180.5	183.8	178.5	181.8
600	300	300	205.3	212.6	200.7	208.1
800	400	400	214.3	227.4	204.0	217.1
780	380	400	214.3	226.7	204.0	216.4
1070	570	500	61.7	85.0	48.6	72.0
1210	610	600	78.7	108.5	62.3	92.1
1485	735	750	108.7	153.6	84.6	129.5
600	400	200	228.7	236.1	224.8	232.1
600	200	400	151.1	158.5	146.5	153.8
1065	465	600	54.6	77.7	41.4	64.5
1070	670	400	53.9	77.2	40.8	64.1
1430	430	1000	100.9	142.5	80.6	122.2
1450	950	500	103.5	146.3	80.6	123.4

pipe. The first 6 columns in Table 5 are self explanatory. Column 7 is the negative of the regression coefficient and represents the slope of the energy line or the head loss divided by the length of pipe. The eighth column contains the regression correlation coefficient squared, i.e. R^2, and as such is a measure of the scatter of the total energy head data from a fitted straight line. At the lower flow rates of 150 and 200 gpm these correlation coefficients are of such small value as to indicate that the computed slope of the energy line is of questionable accuracy. These small values of R^2 are a consequence of the very small head losses at these low flow rates in comparison to the precision with which the data could be recorded using the mercury manometers at separate pipe sections. The ninth, or next to the last column, contains the friction factor f computed from the slope of the energy line and the Darcy-Weisbach equation, i.e.

$$f = \frac{h_L/L}{V^2/(2gd)} \quad . \quad . \quad . \quad . \quad . \quad . \quad . \quad . \quad . \quad . \quad . \quad . \quad (10)$$

The tenth or final column in Table 5 contains the value of the friction factor computed by Prandl's friction equation for hydraulically smooth pipes, Eq. 4.

The close agreement between the friction factor f in the last two columns of Table 5 indicates that 6-inch PERMASTRAN® pipe behaves as hydraulically smooth pipe, at least within the range of flow rates (i.e. Reynolds numbers) used in the tests. These results might have been anticipated since the inside wall of the pipe is polyvinylchloride (plastic) and smooth to the touch. The roughness of this wall material is embedded well within the laminar sublayer and consequently has no influence on the frictional head loss.

As a consequence of this conclusion the head loss in 6-inch PERMASTRAN® (or PVC pipe which has the same inside wall material)

can be computed by,

$$h_L = f \frac{L}{d} \frac{V^2}{2g} \quad . \quad . \quad . \quad . \quad . \quad . \quad . \quad . \quad . \quad . \quad . \quad . \quad (11)$$

in which the friction factor f can be computed from,

$$\frac{1}{\sqrt{f}} = 2 \log_{10} (R_e \sqrt{f}) - 0.8 \quad . \quad . \quad . \quad . \quad . \quad . \quad . \quad . \quad . \quad (4)$$

or by the explicit Blasius Equation

$$f = \frac{.316}{R_e^{.25}} \quad . \quad . \quad . \quad . \quad . \quad . \quad . \quad . \quad . \quad . \quad . \quad . \quad . \quad (3)$$

for values of Reynolds number between 2×10^3 and 1×10^5.

The data from test series No. 6 were obtained with the 4-inch PERMASTRAN® pipe downstream from the 6x6x4-inch tee. The data from this series have been analyzed by the same weighted regression analyses described above to determine the frictional head loss in this 4-inch pipe. A summary of these analyses is given in Table 6. Table 6 has two additional columns that were not included in Table 5. These last two columns give the values of the relative roughness $\frac{e}{d}$ of the wall material and the equivalent sand roughness e, that would result from substituting the friction factor f from column 9 into the Colebrook-White equation

$$\frac{1}{\sqrt{f}} = 1.14 - 2 \log_{10} \left(\frac{e}{d} + \frac{9.35}{R_e \sqrt{f}} \right) \quad . \quad . \quad . \quad . \quad . \quad (5)$$

and computing e/d from this equation. The fact that the equivalent roughness e decreases quite rapidly with increasing flow rates suggests that the reason the computer value of f is slightly larger than the f for hydraulically smooth pipe, at least in part, is due to the precision with which the piezometric heads data can be measured. This conclusion can be justified further on the basis that with the 6-inch outlet of the tee

Table 6. Summary of frictional losses in 4-inch PERMASTRAN® pipe. Diameter, d = 4.23 inches, kinematic viscosity of fluid, $\nu = 1.9 \times 10^{-5}$ ft^2/sec.

Test series No.	Flow rate		Average Velocity (fps)	Velocity Head (ft)	Reynolds No. $\times 10^{-5}$	Slope of energy line h_L/L	Correl. Coef. R^2	Friction factor f	"Smooth pipe" f	Relative roughness e/d	Equivalent roughness e(ft)
	gpm	cfs									
6	50	0.111	1.141	0.0202	0.212	0.0033	0.802	0.05	0.0255		
	100	0.223	2.282	0.0809	0.423	0.00368	0.845	0.0234	0.0217		
	200	0.445	4.564	0.3235	0.847	0.02142	0.985	0.0233	0.0186	0.00127	0.00044
	300	0.668	6.846	0.7279	1.27	0.04158	0.995	0.0201	0.0171	0.00058	0.00021
	400	0.891	9.129	1.294	1.69	0.07058	0.996	0.0191	0.0162	0.00050	0.00016
	500	1.114	11.411	2.022	2.12	0.10248	0.994	0.0178	0.0155	0.00033	0.00011
	577	1.285	13.168	2.693	2.44	0.11751	0.991	0.0153	0.0150	0.00004	0.00001

plugged substantial pressure fluctuations existed in the system causing the mercury columns of the manometer to bounce as much as a couple of inches. With bouncing manometer columns it was extremely difficult to read the values for H_{min} and ΔH accurately even to the nearest tenth of an inch because it was a matter of judgment to decide where the mean values were.

Therefore it is the belief of the writer that 4-inch PERMASTRAN® pipe behaves as hydraulically smooth pipe within the Reynolds number range of tests, despite the fact that the data may suggest that the friction factors lie in the lower portion of the transition region of the Moody diagram. After all there is no reason for 6-inch PERMASTRAN® pipe to be hydraulically smooth and 4-inch PERMASTRAN® pipe with the same wall material to have a large equivalent roughness.

Table 7 gives the head losses as a function of the flow rates for 6-inch PERMASTRAN®, 6-inch PVC, 4-inch PERMASTRAN® and 4-inch PVC pipes. These head losses, expressed in terms of feet loss per 100-feet of pipe length, were computed under the assumption that the pipes behave as hydraulically smooth pipes. A number of measurements of the inside diameter of the pipes indicated the following values:

Internal diameter of 6-inch PERMASTRAN® pipe = 6.25 inches

Internal diameter of 6-inch PVC pipe = 6.09 inches

Internal diameter of 4-inch PERMASTRAN® pipe = 4.23 inches

Internal diameter of 4-inch PVC pipe = 4.13 inches

The head losses in Table 7 assume pipes of the above inside diameters. These same diameters were used in analyzing the test data.

The head losses for these four pipes are shown as a function of the flow rate in Fig. 13.

While the friction factor-Darcy-Weisbach equation approach is the most fundamentally sound method for computing head losses and flow rates in pipes, empirical equations are still frequently used. Two such equations are the Hazen-Williams equation,

Table 7. Head losses in 6-inch and 4-inch PERMASTRAN® and PVC pipes over a range of Reynolds numbers.

Flowrate		6" - PERMASTRAN pipe			6" - PVC pipe			4" - PERMASTRAN pipe			4" - PVC pipe		
(gpm)	(cfs)	R_e	V	$h_L/100'$	R_e	V	$h_L/100'$	R_e	V	$h_L/100'$	R_e	V	$h_L/100'$
50	.111	.224+05	.52	.021	.230+05	.55	.023	.331+05	1.14	.132	.339+05	1.20	.148
100	.223	.447+05	1.05	.070	.459+05	1.10	.079	.661+05	2.28	.451	.677+05	2.39	.505
150	.334	.671+05	1.57	.144	.689+05	1.65	.163	.992+05	3.42	.930	.102+06	3.59	1.043
200	.445	.895+05	2.09	.240	.918+05	2.20	.272	.132+06	4.56	1.559	.135+06	4.79	1.748
250	.557	.112+06	2.61	.358	.115+06	2.75	.405	.165+06	5.71	2.329	.169+06	5.99	2.612
300	.668	.134+06	3.14	.497	.138+06	3.30	.562	.198+06	6.85	3.235	.203+06	7.18	3.629
350	.780	.157+06	3.66	.655	.161+06	3.85	.742	.231+06	7.99	4.273	.237+06	8.38	4.793
400	.891	.179+06	4.18	.833	.184+06	4.40	.944	.264+06	9.13	5.439	.271+06	9.58	6.102
450	1.002	.201+06	4.70	1.030	.207+06	4.95	1.167	.297+06	10.27	6.731	.305+06	10.77	7.552
500	1.114	.224+06	5.23	1.246	.230+06	5.61	1.412	.331+06	11.41	8.147	.339+06	11.97	9.141
550	1.225	.246+06	5.75	1.481	.253+06	6.06	1.677	.364+06	12.55	9.684	.372+06	13.17	10.866
600	1.336	.268+06	6.27	1.733	.275+06	6.61	1.963	.397+06	13.69	11.340	.406+06	14.36	12.724
650	1.448	.291+06	6.79	2.003	.298+06	7.16	2.269	.430+06	14.83	13.114	.440+06	15.56	14.715
700	1.559	.313+06	7.32	2.291	.321+06	7.71	2.595	.463+06	15.98	15.004	.474+06	16.76	16.837
750	1.670	.336+06	7.84	2.596	.344+06	8.26	2.941	.496+06	17.12	17.009	.508+06	17.96	19.088
800	1.782	.358+06	8.36	2.918	.367+06	8.81	3.306	.529+06	18.26	19.128	.542+06	19.15	21.466
850	1.893	.380+06	8.89	3.257	.390+06	9.36	3.690	.562+06	19.40	21.360	.575+06	20.35	23.971
900	2.004	.403+06	9.41	3.613	.413+06	9.91	4.094	.595+06	20.54	23.703	.609+06	21.55	26.601
950	2.116	.425+06	9.93	3.986	.436+06	10.46	4.516	.628+06	21.68	26.156	.643+06	22.74	29.355
1000	2.227	.447+06	10.45	4.375	.459+06	11.01	4.957	.661+06	22.82	28.719	.677+06	23.94	32.232
1050	2.339	.470+06	10.98	4.781	.482+06	11.56	5.417	.694+06	23.96	31.391	.711+06	25.14	35.231
1100	2.450	.492+06	11.50	5.203	.505+06	12.11	5.895	.727+06	25.10	34.170	.745+06	26.33	38.351
1150	2.561	.514+06	12.02	5.641	.528+06	12.66	6.392	.760+06	26.24	37.057	.779+06	27.53	41.592
1200	2.673	.537+06	12.54	6.095	.551+06	13.21	6.907	.793+06	27.39	40.051	.812+06	28.73	44.952
1250	2.784	.559+06	13.07	6.565	.574+06	13.76	7.439	.826+06	28.53	43.150	.846+06	29.93	48.431
1300	2.895	.582+06	13.59	7.051	.597+06	14.31	7.990	.859+06	29.67	46.354	.880+06	31.12	52.028
1350	3.007	.604+06	14.11	7.553	.620+06	14.86	8.559	.892+06	30.81	49.662	.914+06	32.32	55.742
1400	3.118	.626+06	14.64	8.070	.643+06	15.41	9.145	.925+06	31.95	53.074	.948+06	33.52	59.573
1450	3.229	.649+06	15.16	8.603	.666+06	15.96	9.749	.958+06	33.09	56.590	.982+06	34.71	63.520
1500	3.341	.671+06	15.68	9.152	.689+06	16.52	10.371	.992+06	34.23	60.209	.102+07	35.91	67.582
1550	3.452	.693+06	16.20	9.715	.712+06	17.07	11.010						
1600	3.563	.716+06	16.73	10.295	.735+06	17.62	11.666						
1650	3.675	.738+06	17.25	10.889	.758+06	18.17	12.340						
1700	3.786	.761+06	17.77	11.498	.781+06	18.72	13.031						
1750	3.898	.783+06	18.29	12.123	.803+06	19.27	13.739						
1800	4.009	.805+06	18.82	12.763	.826+06	19.82	14.464						
1850	4.120	.828+06	19.34	13.418	.849+06	20.37	15.207						
1900	4.232	.850+06	19.86	14.088	.872+06	20.92	15.966						
1950	4.343	.872+06	20.38	14.772	.895+06	21.47	16.742						
2000	4.454	.895+06	20.91	15.471	.918+06	22.02	17.534						
2050	4.566	.917+06	21.43	16.185	.941+06	22.57	18.344						
2100	4.677	.939+06	21.95	16.914	.964+06	23.12	19.170						
2150	4.788	.962+06	22.48	17.657	.987+06	23.67	20.012						
2200	4.900	.984+06	23.00	18.415	.101+07	24.22	20.872						
2250	5.011	.101+07	23.52	19.188	.103+07	24.77	21.747						
2300	5.122	.103+07	24.04	19.975	.106+07	25.32	22.639						
2350	5.234	.105+07	24.57	20.776	.108+07	25.87	23.548						
2400	5.345	.107+07	25.09	21.592	.110+07	26.42	24.473						
2450	5.457	.110+07	25.61	22.422	.112+07	26.97	25.414						
2500	5.568	.112+07	26.13	23.266	.115+07	27.53	26.371						

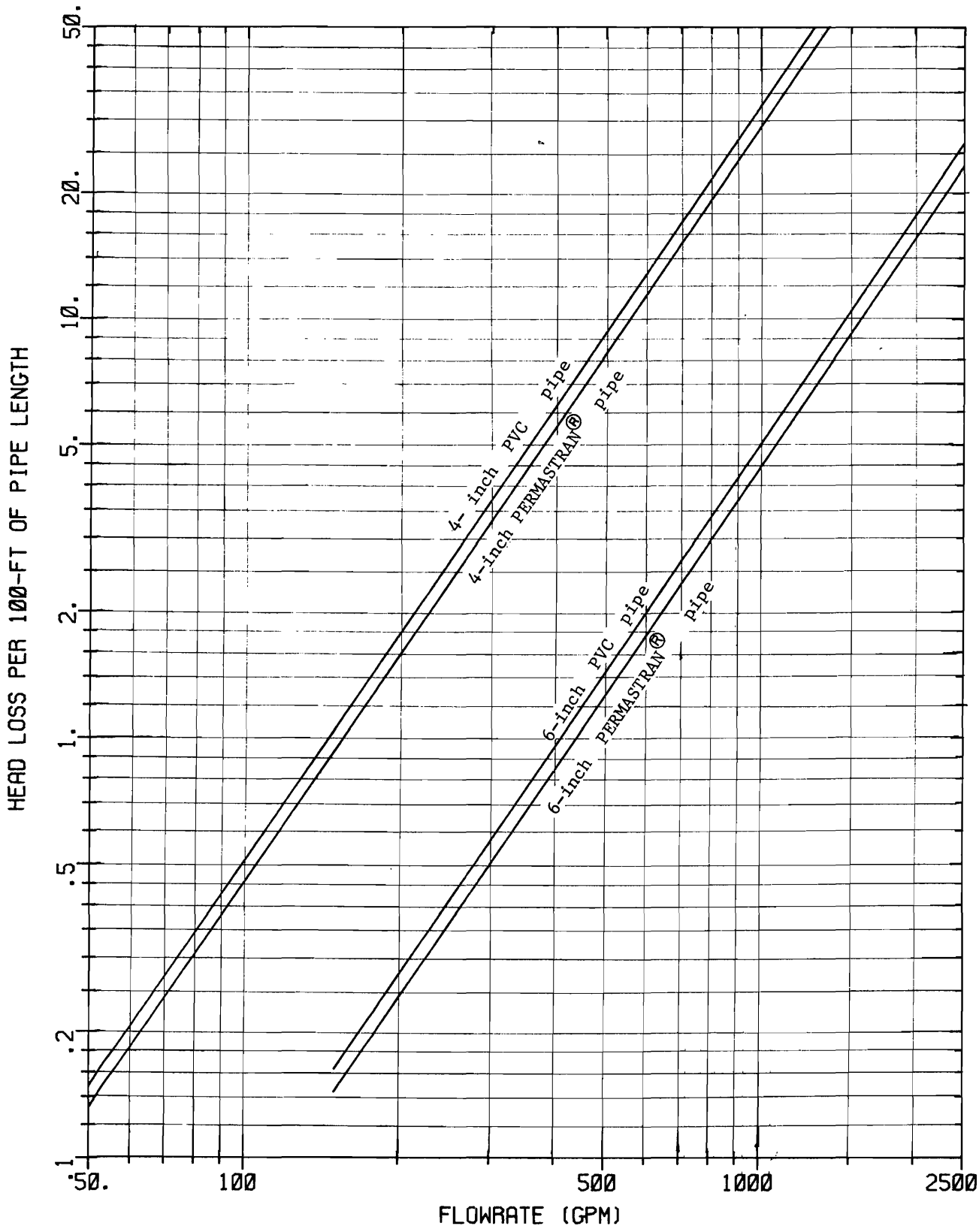

FIG. 13. HEAD LOSS AS A FUNCTION OF THE FLOWRATE IN FOUR DIFFERENT PIPE

$$Q = 1.318CA\left(\frac{d}{4}\right)^{.63} S^{.54} \quad . \quad . \quad . \quad . \quad . \quad . \quad . \quad . \quad (12)$$

and the Manning equation,

$$Q = \frac{1.49}{n} A\left(\frac{d}{4}\right)^{2/3} S^{1/2} \quad . \quad . \quad . \quad . \quad . \quad . \quad . \quad . \quad (13)$$

If the coefficient C and n in these equations are held constant for a given pipe, as is commonly done, the two empirical equations apply only in a limited range of flow velocities. The Hazen-Williams equation indicates the head loss is proportional to the velocity to the 1.85 power, and the Manning equation indicates the head loss is proportional to the velocity squared.

Evaluating the Hazen-Williams coefficient C and the Manning's coefficient n so that they give the same head loss as the Darcy-Weisbach equation for a flow rate of 800 gpm in 6-inch PERMASTRAN® pipe leads to,

$$C = 154.6$$

$$n = .0078$$

Table 8 compares the head loss computed by the Darcy-Weisbach equation under the assumption that the pipes are smooth with the head losses computed by the Hazen-Williams equation and the Manning equation using the above coefficients, over a range of Reynolds numbers. This comparison illustrates that the empirical equations apply over a limited range unless the coefficients are changed depending upon the flow conditions.

Determination of Head Losses at the Elbow and Tees

Elbow Head Loss. The data from test series 1, 2, 3 and 4, obtained from lay-out No. 1, have been used to determine the head losses due to the 6-inch RING-TITE filament wound 90° elbow. The more rapidly moving fluid near the core of the pipe will have a larger centrifugal

Table 8. Comparison of the head losses over a range of Reynolds numbers as determined by: (1) the Darcy-Weisbach method, (2) the Hazen-Williams equation, and (3) the Mannings equation. For the f factor in the Darcy-Weisbach equation, the pipe was assumed hydraulically smooth, the coefficient in the Hazen-Williams equation was taken as C = 154.6, and the coefficient in Mannings equation was taken as n = .0078.

Reynolds Number	6-inch PERMASTRAN PIPE						6-inch PVC PIPE						4-inch PERMASTRAN PIPE						4-inch PVC PIPE					
	Velocity (fps)	Flow-rate (cfs)	friction factor f	head loss/100' $h_{L/100'}$			Velocity (fps)	Flow-rate (cfs)	Friction factor f	head loss/100' $h_{L/100'}$			Velocity (fps)	Flow-rate (cfs)	Friction factor f	head loss/100' $h_{L/100'}$			Velocity (fps)	Flow-rate (cfs)	Friction factor f	head loss/100' $h_{L/100'}$		
				Darcy-Weisb.	Hazen-Will.	Mann-ings				Darcy-Weisb.	Hazen-Will.	Mann-ings				Darcy-Weisb.	Hazen-Will.	Mann-ings				Darcy-Weisb.	Hazen-Will.	Mann-ings
.15+07	35.05	7.47	.0109	39.8	41.6	51.3	35.97	7.28	.0109	43.1	45.0	55.9	51.79	5.05	.0109	128.5	135.1	188.3	53.04	4.93	.0109	138.1	145.2	203.9
.10+07	23.37	4.98	.0116	19.0	19.7	22.8	23.98	4.85	.0116	20.5	21.3	24.8	34.52	3.37	.0116	61.2	63.8	83.7	35.35	3.29	.0116	65.7	68.6	90.6
.90+06	21.03	4.48	.0119	15.6	16.2	18.5	21.58	4.37	.0119	16.9	17.5	20.1	31.07	3.03	.0119	50.4	52.5	67.8	31.82	2.96	.0119	54.2	56.5	73.4
.80+06	18.69	3.98	.0121	12.6	13.0	14.6	19.18	3.88	.0121	13.6	14.1	15.9	27.62	2.70	.0121	40.7	42.2	53.6	28.29	2.63	.0121	43.7	45.4	58.0
.70+06	16.36	3.48	.0124	9.9	10.2	11.2	16.79	3.40	.0124	10.7	11.0	12.2	24.17	2.36	.0124	31.9	33.0	41.0	24.75	2.30	.0124	34.3	35.5	44.4
.60+06	14.02	2.99	.0127	7.5	7.6	8.2	14.39	2.91	.0127	8.1	8.3	8.9	20.71	2.02	.0127	24.1	24.8	30.1	21.22	1.97	.0127	25.9	26.7	32.6
.50+06	11.68	2.49	.0132	5.4	5.5	5.7	11.99	2.43	.0132	5.8	5.9	6.2	17.26	1.68	.0132	17.3	17.7	20.9	17.68	1.64	.0132	18.6	19.0	22.7
.40+06	9.347	1.991	.0137	3.57	3.61	3.64	9.592	1.940	.0137	3.86	3.90	3.97	13.810	1.348	.0137	11.52	11.72	13.39	14.144	1.316	.0137	12.37	12.59	14.50
.35+06	8.178	1.742	.0141	2.80	2.82	2.79	8.393	1.698	.0141	3.03	3.05	3.04	12.084	1.179	.0141	9.04	9.15	10.25	12.376	1.151	.0141	9.71	9.84	11.10
.30+06	7.010	1.493	.0145	2.12	2.12	2.05	7.194	1.455	.0145	2.29	2.29	2.24	10.357	1.011	.0145	6.84	6.88	7.53	10.608	.987	.0145	7.34	7.40	8.16
.25+06	5.842	1.245	.0150	1.52	1.51	1.42	5.995	1.213	.0150	1.65	1.64	1.55	8.631	.842	.0150	4.91	4.91	5.23	8.840	.822	.0150	5.28	5.28	5.67
.20+06	4.673	.996	.0156	1.02	1.00	.91	4.796	.970	.0156	1.10	1.08	.99	6.905	.674	.0156	3.28	3.25	3.35	7.072	.658	.0156	3.53	3.49	3.63
.15+06	3.505	.747	.0166	.61	.59	.51	3.597	.728	.0166	.66	.64	.56	5.179	.505	.0166	1.96	1.91	1.88	5.304	.493	.0166	2.10	2.05	2.04
.10+06	2.337	.498	.0180	.29	.28	.23	2.398	.485	.0180	.32	.30	.25	3.452	.337	.0180	.94	.90	.84	3.536	.329	.0180	1.02	.97	.91
.90+05	2.1030	.4480	.0184	.243	.228	.185	2.1582	.4366	.0184	.262	.247	.201	3.1072	.3032	.0184	.782	.742	.678	3.1825	.2961	.0184	.841	.797	.734
.80+05	1.8693	.3983	.0189	.196	.184	.146	1.9184	.3881	.0189	.212	.199	.159	2.7620	.2695	.0189	.634	.597	.536	2.8289	.2632	.0189	.681	.641	.580
.70+05	1.6356	.3485	.0194	.155	.144	.112	1.6786	.3396	.0194	.167	.155	.122	2.4167	.2359	.0194	.499	.466	.410	2.4753	.2303	.0194	.536	.501	.444
.60+05	1.4020	.2987	.0201	.118	.108	.082	1.4388	.2911	.0201	.127	.117	.089	2.0715	.2022	.0201	.379	.350	.301	2.1216	.1974	.0201	.408	.377	.326
.50+05	1.1683	.2489	.0209	.085	.077	.057	1.1990	.2425	.0209	.092	.083	.062	1.7252	.1685	.0209	.274	.250	.209	1.7680	.1645	.0209	.295	.269	.227
.40+05	.9347	.1991	.0220	.057	.051	.036	.9592	.1940	.0220	.062	.055	.040	1.3810	.1348	.0220	.185	.165	.134	1.4144	.1316	.0220	.198	.178	.145
.35+05	.8178	.1742	.0227	.045	.040	.028	.8393	.1698	.0227	.049	.043	.030	1.2084	.1179	.0227	.146	.129	.103	1.2376	.1151	.0227	.157	.139	.111
.30+05	.7010	.1493	.0235	.034	.030	.021	.7194	.1455	.0235	.037	.032	.022	1.0357	.1011	.0235	.111	.097	.075	1.0608	.0987	.0235	.119	.104	.082
.25+05	.5842	.1245	.0245	.025	.021	.014	.5995	.1213	.0245	.027	.023	.016	.8631	.0842	.0245	.080	.069	.052	.8840	.0822	.0245	.086	.075	.057
.20+05	.4673	.0995	.0259	.017	.014	.009	.4796	.0970	.0259	.018	.015	.010	.6905	.0674	.0259	.054	.046	.033	.7072	.0658	.0259	.058	.049	.036
.15+05	.3505	.0747	.0278	.010	.008	.005	.3597	.0728	.0278	.011	.009	.006	.5179	.0505	.0278	.033	.027	.019	.5304	.0493	.0278	.035	.029	.020
.10+05	.2337	.0498	.0309	.005	.004	.002	.2398	.0485	.0309	.005	.004	.002	.3452	.0337	.0309	.010	.013	.008	.3536	.0329	.0309	.017	.014	.009
.90+04	.2103	.0448	.0318	.004	.003	.002	.2158	.0437	.0318	.005	.003	.002	.3107	.0303	.0318	.014	.010	.007	.3182	.0296	.0318	.015	.011	.007
.80+04	.1869	.0398	.0323	.003	.003	.001	.1918	.0388	.0328	.004	.003	.002	.2762	.0270	.0328	.011	.008	.005	.2829	.0263	.0328	.012	.009	.006
.70+04	.1636	.0348	.0340	.003	.002	.001	.1679	.0340	.0340	.003	.002	.001	.2417	.0236	.0340	.009	.007	.004	.2475	.0230	.0340	.009	.007	.004
.60+04	.1402	.0299	.0355	.002	.002	.001	.1439	.0291	.0355	.002	.002	.001	.2071	.0202	.0355	.007	.005	.003	.2122	.0197	.0355	.007	.005	.003

force than the slower moving fluid adjacent to the pipe wall and consequently the core fluid will move outward in moving around a bend as the outer layers are forced inward. This action results in a double spiral secondary motion in the pipe flow downstream from the bend. As pointed out in the introduction, for bends of large bend radius, this secondary flow may persist for 50 to 100 pipe diameters downstream until eventually viscous action dampens it out. The velocity due to this secondary motion, when superimposed on the main axial velocity, results in a larger total velocity, and consequently more than the usual amount of frictional loss occurs in the pipe downstream from the bend.

Some of the head loss due to the 90^{o} elbow is due to this induced secondary motion. (Even though the test results have indicated this head loss is smaller than the writer had initially anticipated.) The other and major head losses due to the elbow are caused by separation and the added turbulence set up in the fluid as it is rapidly forced to change directions.

The following procedure was used in computing the head losses due to the elbow as well as the tees which are described later. After ascertaining that the pipe (both PVC and PERMASTRAN®) are hydraulically smooth within the range of Reynolds numbers of the tests, it was decided that the slopes of the energy lines both upstream from as well as downstream from the bend should be established as that which would exist in a hydraulically smooth pipe for the given Reynolds number. Because of the scatter in the data the position of this sloping energy line was established by weighting the values for the energy line as determined from the pressure taps. The weightings used are given in Table 9.

Table 9. Weighting factors used to establish position of energy line with a known slope as determined by hydraulically smooth flow.

	Upstream			Downstream							
Section No. of Pressure Tap	1	2	3a	3b	4	5	6	7	8	9	10
Value of Weighting	1	2	1	1	2	3	5	5	5	3	4

The position of the energy lines was computed so that it passed through the center of mass of the weighted values of the energy line as determined from the recorded data. In essence this procedure specified the slope of the line for a weighted regression so that the computed values of the friction factor would exactly equal the value for a "smooth pipe," i.e., this procedure forced the f's in the last two columns of Table 5 to be equal.

After thus establishing the position of both the energy line upstream and downstream from the elbow, the height of the energy lines coming from upstream, and leaving in the downstream direction were computed at the center of the elbow. The difference between these two lines (at the center of the elbow) is the head loss due to the elbow. This determination of head loss is illustrated on Fig. 14, which shows both the upstream energy line and the downstream energy line for two different flow rates as well as the height of the energy head as computed from the pressure taps. The data shown on Fig. 14 actually come from test series No. 5, when the 6x6x6-inch tee was installed in place of the elbow, and consequently the head losses are greater than normally would occur due to the elbow.

A summary of the head losses due to the elbow as determined by the above procedure is given in Table 10 for those tests for which the

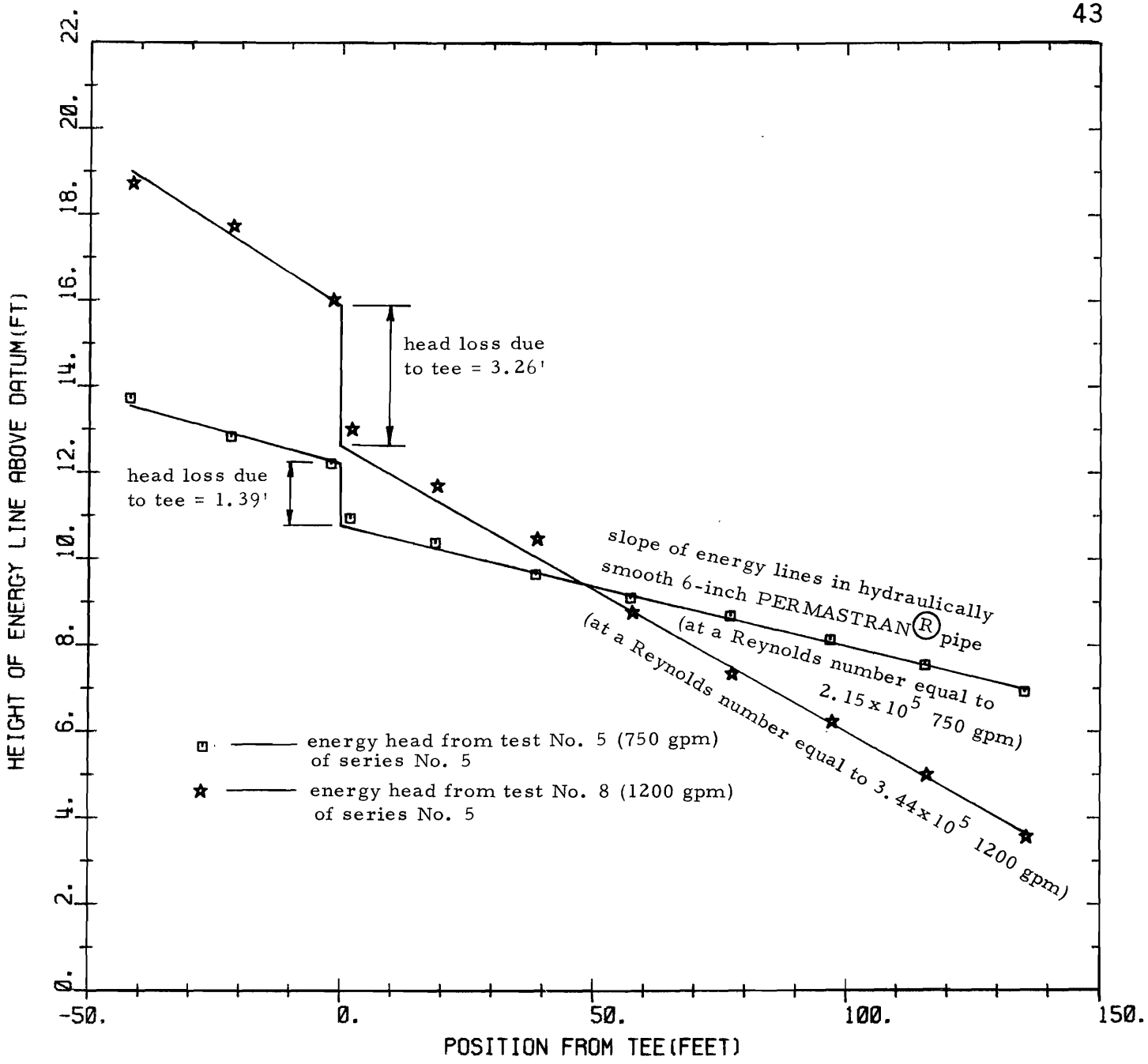

FIG. 14. EXAMPLE OF ENERGY LINE PAST THE 6X6X6 RING TITE TEE WITH THE STRAIGHT THROUGH OUTLET PIPE PLUGGED.

Table 10. Head losses due to the 6-inch 90-degree elbow.

Series No.	Flow rate (gpm)	Velocity (fps)	Velocity Head (ft)	Reynolds Number ($\times 10^{-5}$)	Head loss		Head loss Coeff. C_L
					inches	ft	
1	300	3.136	0.1527	0.860	0.83	0.069	0.45
	400	4.181	0.2715	1.15	1.44	0.120	0.44
	500	5.227	0.4242	1.43	2.27	0.189	0.44
	600	6.272	0.6109	1.72	3.44	0.287	0.47
	731	7.642	0.9067	2.09	5.49	0.457	0.50
2	300	3.136	0.1527	0.860	0.788	0.066	0.43
	600	6.272	0.6109	1.72	2.94	0.245	0.41
	750	7.840	0.9545	2.15	5.77	0.481	0.37
	900	9.408	1.375	2.58	6.40	0.533	0.39
	1200	12.544	2.444	3.44	11.2	0.935	0.38
	1300	13.590	2.868	3.73	14.1	1.175	0.41
3	1200	12.544	2.444	3.44	14.4	1.20	0.49
	900	9.408	1.375	2.58	8.1	0.675	0.49
	750	7.840	0.955	2.15	5.28	0.440	0.46
	600	6.272	0.611	1.72	3.49	0.295	0.48
	1300	13.590	2.868	3.73	15.6	1.30	0.45
4	400	4.181	0.2715	1.15	1.89	0.157	0.58
	500	5.227	0.4242	1.43	3.10	0.258	0.61
	600	6.272	0.6109	1.72	4.18	0.348	0.57
	750	7.840	0.955	2.15	6.87	0.572	0.60
	900	9.408	1.375	2.58	8.73	0.728	0.53
	1200	12.544	2.444	3.44	15.43	1.29	0.53
						Av.	0.49

elbow was in the pipe line. Since the values at the higher flow rates are probably more reliable than those at the lower flow rates (the error in reading the mercury manometer for the low flow rates is a sizable percent of the head loss, whereas at the higher flow rates where the losses are much greater the error is still approximately the same and therefore the percentage error is smaller), the writer recommends that the head loss coefficient C_L for the elbow should equal 0.5. This coefficient is defined by the equation,

$$h_L = C_L \frac{V^2}{2g} \quad . \quad . \quad . \quad . \quad . \quad . \quad . \quad . \quad . \quad . \quad . \quad (14)$$

in which the velocity is the average velocity in the PERMASTRAN® pipe downstream from the elbow.

This coefficient should probably vary slightly depending upon how far the pipes are fitted into the elbow. The RING-TITE filament wound 90^o elbow does not have any notches which establish the position to which the pipes should be inserted into the elbow ends. In running the tests the pipes were inserted 4 3/4 inches into the elbow.

Because of the accuracy of the original recorded data the head losses in Table 10 are not good to the two digits beyond the decimal point as recorded in the inches column. The original data are probably good only to the nearest inch. This accuracy explains much of the variation in the computed head loss coefficient in the last column of Table 10.

RING-TITE 6 x 6 x 6-Inch Tee with Extension Pipe Plugged. Data from test series No. 5 have been used to determine the head losses due to the 6 x 6 x 6-inch RING-TITE filament wound tee operating with the flow entering one of the "straight through" branches of the tee and being turned through 90^o. The test lay-out for this series of tests is illustrated in Fig. 6.

The same procedure has been used to analyze this data in determining the head losses due to the tee as the procedure explained in the previous section for the 90^o elbow. The slopes of the energy lines both upstream and downstream from the tee were determined to fit the total head data best and simultaneously have the slope that would exist for a hydraulically smooth pipe.

The results from these analyses are summarized in Table 11. The average loss coefficient from the 8 tests with flow rates from 300 to 1200 gpm equal 1.69. The data tend to suggest that the head loss coefficient

Table 11. Head losses due to the 6x6x6-inch tee operating with the "straight through" outlet pipe plugged.

Flow rate (gpm)	Velocity (fps)	Velocity Head (ft)	Reynolds Number ($\times 10^{-5}$)	Head loss		Head loss Coefficient C_L
				inches	feet	
300	3.136	0.1527	0.86	3.97	0.331	2.17
400	4.181	0.2715	1.15	6.77	0.564	2.08
500	5.227	0.4242	1.43	11.2	0.930	2.19
600	6.272	0.6109	1.72	10.2	0.850	1.40
750	7.840	0.9545	2.15	16.6	1.39	1.45
900	9.408	1.374	2.65	24.5	2.04	1.48
1050	10.976	1.871	3.09	31.7	2.64	1.41
1200	12.544	2.444	3.44	39.2	3.26	1.36
					Av.	1.69

might be larger for the lower flow rates. The accuracy of the data, particularly since sizable pressure fluctuations occur in the tee operating in this mode, cannot fully support this conclusion, however. The writer suggests a head loss coefficient C_L equal to 1.5 be used to compute the head loss for the tee operating with the "straight through" pipe plugged.

RING-TITE 6x6x4-Inch Tee with 6-Inch Extension Pipe Plugged. Data from test series No. 6 have been used to determine the head losses due to the 6x6x4-inch RING-TITE filament wound tee operating with the flow entering one of the 6-inch "straight through" branches of the tee and leaving at 90° therefrom through the 4-inch branch. This same data were analyzed to also determine the frictional losses in 4-inch PERMASTRAN® pipe.

In determining the head losses due to the tee, the procedure of establishing the position of the energy lines upstream and downstream from the tee, which was described earlier, was used. For this test lay-out only 4, 20-foot sections of 4-inch PERMASTRAN® pipe were available, and therefore it was necessary that the last three sections

of 20-foot pipe be 4-inch PVC pipe. The I.D. of the 4-inch PERMASTRAN® pipes equal 4.23 inches, whereas the I.D. of the PVC pipe equal 4.13 inches. Consequently in establishing the position of the downstream energy line, not only was the difference in velocity heads in the two different pipes taken into account, but also the two different slopes of the energy lines were used in the data fitting procedure.

Table 12 summarizes the head losses due to the 6x6x4-inch tee in the mode of operation of test lay-out No. 3 (Fig. 7). The last two columns in Table 12 contain (a) the head loss coefficient based on the velocity head in the upstream 6-inch pipe, and (b) the head loss coefficient based on the velocity head in the downstream 4-inch pipe. Values suggested for these two loss coefficients are:

$$C_{L_1} = 6.9$$

$$C_{L_2} = 1.6$$

RING-TITE 6x6x6-Inch Tee Operating with One Inflow and Two Outflows. The second mode of operation of the 6x6x6-inch tee was to have the flow entering the tee from one branch of the "straight through" portion and divide this flow into two outflows. This type of operation is depicted in Fig. 3 and the test lay-out used for obtaining the data is shown in Fig. 8 (lay-out No. 4). The data obtained from this test lay-out are referred to as test series No. 7 and the piezometric head and total energy head data from this test series are given in Table 2. This series consisted of nine tests. Seven of these nine tests divided the flow equally (or approximately equally) between the two outflows. The total flow for these seven tests was varied from 200 gpm to 1500 gpm. The additional two tests maintained the total flow at 1200 gpm and varied the outflow through the 90° branch, from 200 gpm to 400 gpm. Combining these two tests with the 1200 gpm - 600 gpm test of the earlier seven

Table 12. Head losses due to the 6x6x4-inch tee operating with the "straight through" outlet pipe plugged.

Flow rate (gpm)	Upstream Velocity (fps)	Downstream Velocity (fps)	Upstream Vel. Head (ft)	Downstream Vel. Head (ft)	Head loss		Head loss Coefficients	
					inches	feet	C_{L_1}	C_{L_2}
50	0.551	1.414	0.0047	0.0202	0.5	0.043		
100	1.101	2.282	0.0188	0.0809	1.4	0.12	6.3	1.48
200	2.202	4.564	0.0753	0.3235	6.3	0.52	7.0	1.62
300	3.303	6.846	0.1694	0.7279	17.2	1.43	8.4	1.97
400	4.404	9.129	0.3012	1.294	24.9	2.07	6.9	1.60
500	5.505	11.411	0.4706	2.022	38.1	3.18	6.8	1.57
577	6.353	13.168	0.6267	2.693	48.5	4.04	6.4	1.50
						Av	6.9	1.62

tests gives a subseries in which the effects of different flow divisions on the loss coefficients can be determined. The data from this series of tests have been used only for determining the minor losses due to the 6x6x6-inch tee even though they might also have been used to verify the frictional loss in the 6-inch PERMASTRAN® pipe.

In this series of tests, data from two pressure taps upstream from the tee were obtained. Data from four pressure taps in the downstream "straight through" direction were obtained, and data from seven pressure taps from the downstream "90°" direction were obtained making a total of 13 data values for each test.

With the tee operating in this mode, two different head losses occur. One of these head losses occurs between the flow coming into the tee and the flow leaving the tee in the "straight through" direction. The other head losses occur between the flow coming into the tee and the flow leaving the tee through the other outlet in a 90° direction from the direction of the inflow. In addition to these different losses, the loss coefficients can be defined by dividing the head losses by either the velocity head of the inflow or the velocity head of the outflow. Also a mean head loss coefficient can be defined as discussed later. In order to distinguish the various variables involved in this flow the following subscript notation is adopted:

(a) A subscript 1 denotes the inflow section (thus Q_1 is the total flow entering the tee)

(b) A subscript 2 denotes the "straight through" outflow section, and

(c) A subscript 3 denotes the "90°" outflow section.

Thus Q_1 equals the sum of Q_2 and Q_3. The two different head losses will be denoted $h_{L_{1-2}}$ between sections 1 and 2 and $h_{L_{1-3}}$ between sections 1 and 3.

The head losses were determined by means of the same procedure described earlier for fitting the total energy head data to straight lines

with slopes equal to those computed as the gradient from a hydraulically smooth flow. Three such energy lines were fitted for each test and the difference in the elevations of the inflow energy line, extrapolated to the center of the tee, and the two outflow energy lines equal the two head losses mentioned above. The fitting of these lines weighted the energy head data according to the values in Table 13.

Table 13. Weighting factors used to establish the position of the energy lines entering and leaving the 6 x 6 x 6-inch tee operating with one inflow and two outflows.

	Up-stream		Downstream "straight through"				Downstream "90° direction"						
Section No. of Pressure Tap	1	2	3	4	5	6	7	8	9	10	11	12	13
Value of Weighting	1	3	4	6	4	1	3	8	5	5	4	3	1

A summary of the head losses and head loss coefficients obtained from these fitted energy lines is contained in Table 14. In Table 14, two separate head loss coefficients are given to define each of the two head losses. The coefficients C_{L_1} and C_{L_2} define the head loss between the incoming flow and the flow leaving in the "straight through" direction; C_{L_1} is based on the velocity head of the incoming flow and C_{L_2} is based on the velocity head of the outflow in the "straight through" pipe. The coefficients C_{L_3} and C_{L_4} define the head loss between the incoming flow and the flow leaving in the pipe at 90° from this direction. The coefficient C_{L_3} is based on the incoming velocity head and C_{L_4} is based on the velocity head of the flow leaving in the pipe at 90° from this direction.

In addition a mean head loss h_{L_m} has been defined by,

$$h_{L_m} = h_{L_{1-2}} \frac{Q_2}{Q_1} + h_{L_{1-3}} \frac{Q_3}{Q_1} \quad . \quad . \quad . \quad . \quad . \quad . \quad (15)$$

Table 14. Head losses due to the 6x6x6-inch tee operating with Q_1 entering one "straight through" branch and being divided into two outflows Q_3 at 90° therefrom and Q_2 out other "straight through" branch of the tee.

Flow Rates (gpm)			Velocities (fps)			Velocity Heads (ft)			Reynolds No. x 10^{-5}			Head Losses				Head Loss Coefficients					Mean Head Loss (ft)
												$h_{L_{1-2}}$		$h_{L_{1-3}}$		$C_{L_1}=\frac{h_{L_{1-2}}}{V_1^2/2g}$	$C_{L_2}=\frac{h_{L_{1-2}}}{V_2^2/2g}$	$C_{L_3}=\frac{h_{L_{1-3}}}{V_1^2/2g}$	$C_{L_4}=\frac{h_{L_{1-3}}}{V_3^2/2g}$	C_{L_m}	
Q_1	Q_2	Q_3	V_1	V_2	V_3	$\frac{V_1^2}{2g}$	$\frac{V_2^2}{2g}$	$\frac{V_3^2}{2g}$	R_1	R_2	R_3	inches	ft	inches	ft						h_{L_m}
200	100	100	2.202	1.101	1.045	0.0753	0.0188	0.0170	0.588	0.294	0.287	1.0	0.083	1.94	0.162	1.10	4.41	2.15	9.52	1.63	0.123
400	200	200	4.404	2.202	2.091	0.3012	0.0753	0.0679	1.18	0.588	0.573	1.81	0.151	5.31	0.443	0.50	2.00	1.47	6.52	0.99	0.297
600	300	300	6.606	3.303	3.136	0.678	0.169	0.153	1.76	0.882	0.860	2.51	0.209	11.12	0.927	0.31	1.24	1.37	6.07	0.84	0.568
800	400	400	8.808	4.404	4.181	1.205	0.301	0.272	2.35	1.18	1.15	4.11	0.342	18.27	1.52	0.28	1.14	1.26	5.61	0.77	0.931
1000	500	500	11.01	5.505	5.227	1.882	0.471	0.424	2.94	1.47	1.43	5.41	0.451	29.18	2.43	0.24	0.96	1.29	5.73	0.76	1.44
1200	600	600	13.21	6.61	6.27	2.711	0.678	0.611	3.53	1.76	1.72	6.41	0.53	41.4	3.45	0.20	0.79	1.27	5.65	0.73	1.99
1500	765	735	16.52	8.42	7.68	4.235	1.102	0.917	4.41	2.25	2.11	7.49	0.62	61.83	5.15	0.15	0.57	1.22	5.62	0.68	2.89
1200	1000	200	13.212	11.01	2.091	2.711	1.882	0.0679	3.53	2.94	5.73	13.3	1.11	44.1	3.67	0.41	0.59	1.36	54.1	0.57	1.54
1200	800	400	13.212	8.81	4.18	2.711	1.205	0.2715	3.53	2.35	1.15	4.93	0.411	36.9	3.07	0.15	0.34	1.13	11.3	0.48	1.30
1200	600	600	13.21	6.61	6.27	2.71	0.678	0.611	3.53	1.76	1.72	6.41	0.53	41.4	3.45	0.20	0.79	1.27	5.65	0.73	1.94

Values for this mean head loss are given in the last column of Table 14. From this mean head loss, a mean head loss coefficient C_{L_m} has been defined by,

$$C_{L_m} = \frac{h_{L_m}}{\frac{V_1^2}{2g}} \quad . \quad . \quad . \quad . \quad . \quad . \quad . \quad . \quad . \quad . \quad . \quad (16)$$

Substituting the head losses in terms of their coefficients into Eq. 15, leads to,

$$C_{L_m} \frac{V_1^2}{2g} = C_{L_{1-2}} \frac{V_2^2}{2g} \left(\frac{A_2 V_2}{A_1 V_1}\right) + C_{L_{1-3}} \frac{V_3^2}{2g} \left(\frac{A_3 V_3}{A_1 V_1}\right)$$

$$. \quad . \quad . \quad . \quad . \quad . \quad . \quad . \quad . \quad . \quad (17a)$$

or

$$C_{L_m} = C_{L_{1-2}} \left(\frac{V_2}{V_1}\right)^3 \left(\frac{A_2}{A_1}\right) + C_{L_{1-3}} \left(\frac{V_3}{V_1}\right)^3 \left(\frac{A_3}{A_1}\right) \quad . \quad . \quad (17b)$$

An examination of these head loss coefficients shows that their magnitudes decrease with increasing flow rate or Reynolds number. This trend is significant enough that it cannot be attributable entirely to lack of precision of the pressure tap data at the lower flow rates. The previous tests on the 6 x 6 x 6-inch tee show some decrease of the head loss coefficient with increasing flow rate, but the trends were slight and considering how much an error of 0.05 inch in reading the mercury manometer could effect the magnitude of the head loss coefficient at the lower flow rates, there was insufficient justification to define a relationship of the head loss coefficient with Reynolds number. The data for the tee operating with one inflow and two outflows do justify establishing such a relationship, however. Fig. 15 shows the values of the five head loss coefficients in Table 14 plotted against the

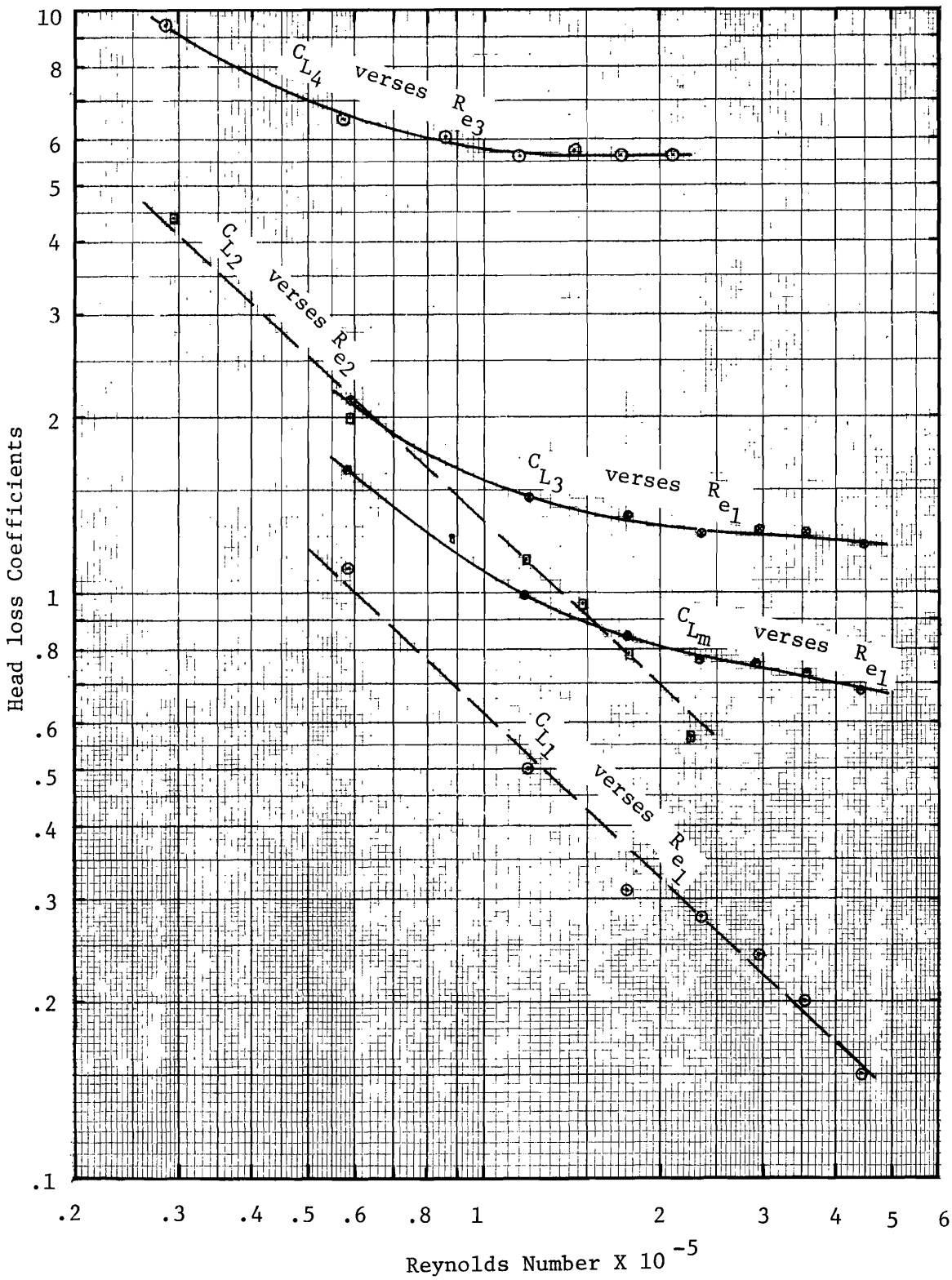

Fig. 15. Head Loss Coefficients due to the 6X6X6-inch tee operating to separate one inflow into two outflows plotted against Reynolds numbers. The two outflows Q_2 and Q_3 are equal.

Reynolds number associated with the velocity in the velocity head used in defining the particular coefficient, as well as the curves fit to this data by eye. This figure can be used to determine the head loss coefficient for the tee operating so that the inflow is divided equally to the two outflow branches.

Fig. 15 shows that the data for the two head loss coefficients C_{L_1} and C_{L_2} for the flow in the "straight through" branch of the tee define straight lines on the log-log plot. The empirical equations for these two lines are:

$$C_{L_1} = \frac{0.62}{(R_e \times 10^{-5})^{.94}} \quad . \quad . \quad . \quad . \quad . \quad . \quad . \quad . \quad . \quad . \quad (18a)$$

$$C_{L_2} = \frac{1.32}{(R_e \times 10^{-5})^{.94}} \quad . \quad . \quad . \quad . \quad . \quad . \quad . \quad . \quad . \quad . \quad (18b)$$

The coefficients C_{L_3} and C_{L_4} associated with the flow in the "90°" outlet branch of the tee as well as the mean head loss coefficient show a definite dependency on Reynolds number, but these relationships do not plot as a straight line on log-log paper. It appears in each case that the head loss coefficients approach a constant value at large Reynolds numbers. The line for C_{L_4} on Fig. 15 shows C_{L_4} equal to 5.6 for Reynolds numbers larger than 1.5×10^5, and C_{L_3} equal to approximately 1.2 for Reynolds numbers larger than 4×10^5.

RING-TITE 6x6x6-Inch Tee Operating to Combine Two Inflows into One Outflow. The third mode of operation of the 6x6x6-inch tee consisted of flow coming into one of the "straight through" branches and the "90°" branch and being combined as outflow from the other "straight through" branch. This mode of operation is given in Fig. 4 and the lay-out for the tests is illustrated in Fig. 9. The data obtained from this

test lay-out are denoted as series No. 8 in Table 2. The lay-out for this series had 6-inch PERMASTRAN® pipe as the pipe containing the combined discharge, a 6-inch PERMASTRAN® pipe carried the flow into the "straight through" branch but a 6-inch PVC pipe conveyed the flow into the 90° branch of the tee. The magnetic flow meter was used to establish the flow rate into the "90°" branch of the tee, and the 3-inch venturi meter was used to measure the entire combined flow for the lower flow rates within its capacity. For the large flow rates the total discharge water was directed into the weighing tanks for measurement. For these larger flow rates it was quite time consuming to establish exactly preselected flow rates. Consequently, the flow entering from the two inlet branches for the higher flow rates are only approximately equal for those tests which were made with the intent of having equal flow rates in these two branches.

The data from this series of tests were used to determine the head losses and head loss coefficients as before by using a weighted fitting of the data to energy head data with the slope determined by hydraulically smooth flow. The weightings used in this fitting process are given in Table 15.

Table 15. Weighting factors used to establish the position of the energy lines entering and leaving the 6x6x6-inch tee operating with two inflows which are combined into a single outflow through one of the "straight through" branches.

	Upstream 90° branch		Upstream "straight through" branch		Downstream "straight through" branch						
Section No. of Pressure Tap	1	2	3	4	5	6	7	8	9	10	11
Value of Weighting	1	3	1	3	3	8	6	4	3	1	1

As in the previous test series No. 7 the data can be used to compute two different head losses; the head loss between each of the two inlets and the outlet. To denote these separate flows the "straight through" inlet branch will be denoted by a 1-subscript. A 2-subscript will denote the outlet branch which contains the combined flow and the "90°" inlet branch will be denoted by a 3-subscript. Thus for this series of tests,

$$Q_2 = Q_1 + Q_3 \quad . \quad . \quad . \quad . \quad . \quad . \quad . \quad . \quad . \quad . \quad . \quad (19)$$

The two head losses for each test will be denoted by $h_{L_{1-2}}$ and $h_{L_{3-2}}$. Each of these head losses might be divided by its inflow velocity head or the outflow velocity head. These four head loss coefficients are given by

$$C_{L_1} = \frac{h_{L_{1-2}}}{V_1^2/2g} \quad . \quad . \quad . \quad . \quad . \quad . \quad . \quad . \quad . \quad . \quad . \quad (20)$$

$$C_{L_2} = \frac{h_{L_{1-2}}}{V_2^2/2g} \quad . \quad . \quad . \quad . \quad . \quad . \quad . \quad . \quad . \quad . \quad . \quad (21)$$

$$C_{L_3} = \frac{h_{L_{3-2}}}{V_3^2/2g} \quad . \quad . \quad . \quad . \quad . \quad . \quad . \quad . \quad . \quad . \quad . \quad (22)$$

$$C_{L_4} = \frac{h_{L_{3-2}}}{V_2^2/2g} \quad . \quad . \quad . \quad . \quad . \quad . \quad . \quad . \quad . \quad . \quad . \quad (23)$$

The head loss coefficients C_{L_2} and C_{L_4} are often referred to as energy transfer coefficients, particularly when dealing with hydraulic manifolds. A summary of these head losses and loss coefficients is contained in Table 16.

Table 16. Head losses due to the 6x6x6-inch tee operating with Q_1 entering one "straight through" branch, Q_3 entering the "90°" branch and being combined into Q_2 which leaves the tee through the other "straight through" branch.

Flow Rates (gpm)			Velocities (fps)			Velocity Heads (ft)			Reynolds No. x 10^{-5}			Head Losses (inches)		Head Losses (feet)		Head Loss Coefficients					Combined Head Loss (ft)
Q_1	Q_3	Q_2	V_1	V_3	V_2	$\frac{V_1^2}{2g}$	$\frac{V_3^2}{2g}$	$\frac{V_2^2}{2g}$	R_{e_1}	R_{e_3}	R_{e_2}	$h_{L_{1-2}}$	$h_{L_{3-2}}$	$h_{L_{1-2}}$	$h_{L_{3-2}}$	$C_{L_1}=\frac{h_{L_{1-2}}}{V_1^2/2g}$	$C_{L_2}=\frac{h_{L_{1-2}}}{V_2^2/2g}$	$C_{L_3}=\frac{h_{L_{3-2}}}{V_3^2/2g}$	$C_{L_4}=\frac{h_{L_{3-2}}}{V_2^2/2g}$	C_{L_m}	h_{L_m}
100	100	200	1.045	1.101	2.091	0.0170	0.0188	0.0679	0.287	0.294	0.573	1.63	1.62	0.14	0.13	8.0	2.0	7.2	2.0	2.0	0.13
200	200	400	2.091	2.202	4.181	0.0679	0.0753	0.2715	0.573	0.588	1.15	1.90	1.26	0.16	0.10	2.3	0.6	1.4	0.4	0.5	0.13
300	300	600	3.136	3.303	6.272	0.1527	0.1694	0.6109	0.860	0.882	1.72	3.60	2.58	0.30	0.21	2.0	0.5	1.3	0.4	0.42	0.26
380	400	780	3.97	4.404	8.15	0.245	0.301	1.032	1.09	1.18	2.24	5.43	5.32	0.45	0.44	1.8	0.4	1.5	0.4	0.43	0.45
570	500	1070	5.96	5.31	11.19	0.551	0.471	1.943	1.63	1.47	3.07	11.1	9.23	0.93	0.77	1.7	0.5	1.6	0.4	0.44	0.85
610	600	1210	6.38	6.61	12.65	0.631	0.678	2.484	1.75	1.76	3.47	13.3	12.3	1.11	1.03	1.7	0.4	1.5	0.4	0.43	1.07
735	750	1485	7.68	8.26	15.824	0.917	1.06	3.742	2.11	2.21	4.26	20.3	17.9	1.69	1.49	1.8	0.4	1.4	0.4	0.43	1.59
400	200	600	4.18	2.20	6.27	0.272	0.0753	0.611	1.15	0.588	1.72	4.25	2.52	0.35	0.21	1.3	0.6	2.8	0.3	0.5	0.31
200	400	600	2.09	4.40	6.27	0.0679	0.3012	0.611	0.573	1.18	1.72	2.87	4.81	0.24	0.40	3.5	0.4	1.3	0.7	0.56	0.35
465	600	1065	4.86	6.61	11.13	0.367	0.678	1.925	1.33	1.76	3.05	7.08	12.0	0.59	1.0	1.6	0.3	1.5	0.5	0.43	0.82
670	400	1070	7.00	4.40	11.19	0.762	0.301	1.943	1.92	1.18	3.07	6.13	3.98	0.51	0.33	0.7	0.3	1.1	0.2	0.23	0.44
430	1000	1430	4.50	11.01	14.95	0.314	1.88	3.47	1.23	2.94	4.10	15.0	26.0	1.25	2.17	4.0	0.4	1.2	0.6	0.55	1.89
950	500	1450	9.93	5.51	15.16	1.53	0.47	3.57	2.72	1.47	4.16	16.0	4.4	1.34	0.36	0.9	0.4	0.8	0.1	0.28	1.00

It is useful to consider the energy for the combined flow. The energy head, while it does have units of length, is actually the energy in ft-lb/sec divided by the weight flow rate in lb/sec. Thus the combined energy of the outflow equals (assuming no loss),

$$\text{combined energy} = \gamma Q_1 E_1 + \gamma Q_3 E_3 \quad . \quad . \quad . \quad . \quad . \quad (24)$$

and the combined energy head can be obtained by dividing the combined energy by the total weight flow rate γQ_2. Since γ is constant for water, the combined energy head is,

$$E_m = E_1 \frac{Q_1}{Q_2} + E_3 \frac{Q_3}{Q_2} \quad . \quad . \quad . \quad . \quad . \quad . \quad . \quad . \quad (25)$$

Consistent with the definition of head losses ($h_{L_{1-2}} = E_1 - E_2$ and $h_{L_{3-2}} = E_3 - E_2$), the combined head loss can be defined as,

$$h_{L_m} = E_m - E_2$$

or

$$h_{L_m} = E_1 \frac{Q_1}{Q_2} + E_3 \frac{Q_3}{Q_2} - E_2 \quad . \quad . \quad . \quad . \quad . \quad (26)$$

If E_1 and E_3 in Eq. 26 are replaced by their equivalents from the definitions of $h_{L_{1-2}}$ and $h_{L_{3-2}}$ and the result simplified, the following equation results,

$$h_{L_m} = h_{L_{1-2}} \frac{Q_1}{Q_2} + h_{L_{3-2}} \frac{Q_3}{Q_2} \quad . \quad . \quad . \quad . \quad . \quad (27)$$

A combined head loss coefficient can be defined by,

$$C_{L_m} = \frac{h_{L_m}}{\frac{V_2^2}{2g}} \quad . \quad . \quad . \quad . \quad . \quad . \quad . \quad . \quad . \quad . \quad . \quad (28)$$

If the head losses in Eq. 27 are replaced by the products of the appropriate head loss coefficient and velocity head the following equation results,

$$C_{L_m} \frac{V_2^2}{2g} = C_{L_1} \frac{V_1^2}{2g} \left(\frac{Q_1}{Q_2}\right) + C_{L_2} \frac{V_3^2}{2g} \left(\frac{Q_3}{Q_2}\right) \quad . \quad . \quad . \quad . \quad . \quad . \quad . \quad . \quad . \quad (29)$$

or

$$C_{L_m} = C_{L_1} \left(\frac{V_1}{V_2}\right)^3 \left(\frac{A_1}{A_2}\right) + C_{L_2} \left(\frac{V_3}{V_2}\right)^3 \left(\frac{A_3}{A_2}\right) \quad . \quad . \quad . \quad . \quad . \quad . \quad . \quad . \quad . \quad (30)$$

There is a great deal of similarity between Eq. 30 and Eq. 18 for the case in which one inflow is separated into two outflows, particularly since in Eq. 18 V_1 represents the velocity in the pipe containing the total flow and V_2 in Eq. 30 is the velocity in the pipe containing the combined flow.

The last two columns in Table 16 contain, respectively, the values of the combined head loss coefficients as computed from either Eq. 28 or Eq. 30, and the combined head loss as computed from Eq. 26.

The head loss coefficients resulting from the tee in this mode of operation of combining two inflows decrease in magnitude with increasing Reynolds number but soon approaches a constant value. Fig. 16 is a log-log plot of the head loss coefficients against the Reynolds number which is associated with the velocity head used in the definition of the particular coefficient. Only the head loss coefficient from the first 7 tests in Table 16 for which the two inlet branches contained equal or near equal flow are plotted in Fig. 16.

A somewhat surprising result is that the head losses and head loss coefficients between the "straight through" inlet branch and the outlet

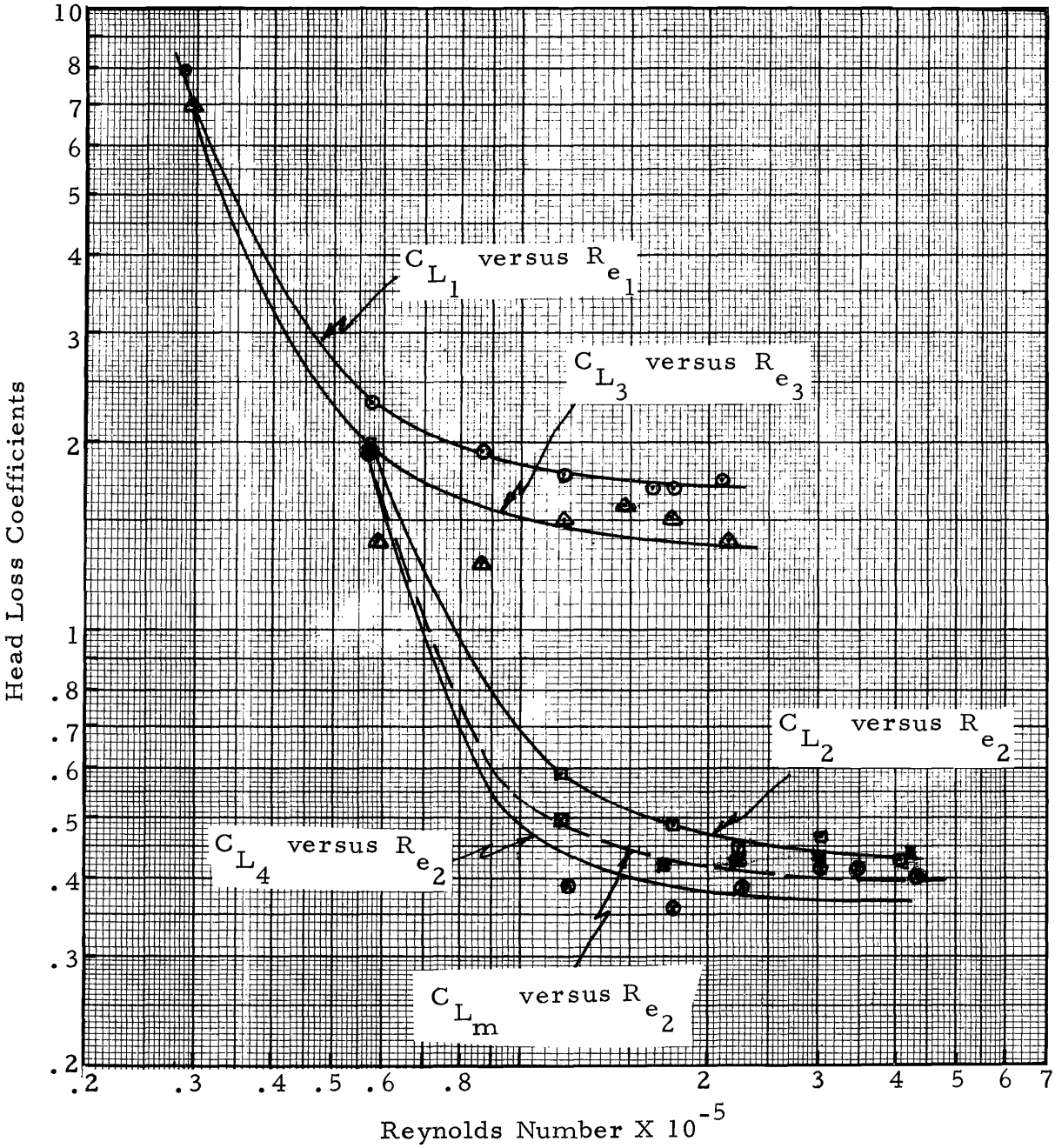

Fig. 16. Head loss coefficients due to the 6x6x6-inch tee operating to combine two inflows into a single outflow through a "straight through branch" plotted against Reynolds numbers. The two inflows Q_1 and Q_3 are equal or approximately equal.

are slightly larger than those associated with the "90°" branch, for these tests with two equal inflows. Clearly much smaller head losses would occur between the "straight through" branches than between the "90°" branch and a "straight through" branch if only a single inflow exists. However, since the outflow contains the mixed fluid from both inlet branches, and the flow field in and around this region of mixing is very complex, this result is not at variance with theory.

Using the energy, momentum and continuity principles, Blaisdell and Manson (1963) give the following two theoretical equations to compute the head losses C_{L_2} and C_{L_4} (the energy transfer coefficients) that would result from sharp-edged pipe junctions of different sizes and angles of junction:

$$C_{L_2} = 2\frac{Q_3}{Q_2} - \left(1+2\frac{A_2}{A_3}\cos\theta\right)\left(\frac{Q_3}{Q_2}\right)^2 \quad . \quad . \quad . \quad . \quad . \quad . \quad (31a)$$

$$C_{L_4} = -1+4\frac{Q_3}{Q_2} - \left[2+2\frac{A_2}{A_3}\cos\theta - \left(\frac{A_2}{A_3}\right)^2\right]\left(\frac{Q_3}{Q_2}\right)^2 \quad . \quad . \quad . \quad (32a)$$

in which the Q's are the flow rates, the A's are the cross-section areas of the pipes and θ is the angle between the two pipes containing the two inflows which equals 90° for a tee. For the tee and test arrangement used these equations reduce to,

$$C_{L_2} = 2\frac{Q_3}{Q_2} - \left(\frac{Q_3}{Q_2}\right)^2 \quad . \quad . \quad . \quad . \quad . \quad . \quad . \quad . \quad . \quad (31b)$$

$$C_{L_4} = -1+4\frac{Q_3}{Q_2} - .9467\left(\frac{Q_3}{Q_2}\right)^2 \quad . \quad . \quad . \quad . \quad . \quad (32b)$$

For equal flow in the two inlet branches, $C_{L_2} = 0.75$ and $C_{L_4} = 0.763$, which show that theory does not predict substantially small coefficients for the head loss between the two "straight through" branches.

These theoretical coefficients correspond with those determined experimentally for the 6 x 6 x 6-inch tee at the Reynolds number of 1×10^5. The fact that the experimental coefficients are less than the theoretical values at higher Reynolds numbers can be explained on the basis that the tee being rounded does reduce the region of separation and amount of turbulence over that of sharp-edged junctions.

The last six lines in Table 16 give head losses from test series No. 8 in which the two inflows are not equal, as is the case for the first seven tests in this table. Fig. 17 shows a plot of the head loss coefficients C_{L_2} and C_{L_4} from these last six tests (the energy transfer coefficients) against the ratio of the flowrates Q_3/Q_2, i.e. the inflow from the "90°" branch divided by the combined flow. Also on this figure, as dashed lines, the theoretical head loss coefficients as computed by Eqs. 31b and 32b for sharp junctions has been plotted.

The experimental data show no change in the head loss coefficients C_{L_2} with the division of flow from the two inlet branches, whereas the coefficient C_{L_4} does increase in value as a large portion of the flow comes through this "90°" branch. The value for the head loss coefficient C_{L_2} (for the "straight through" branch) is approximately equal to 0.4. The head loss coefficient C_{L_4} (for the "90°" branch) can be defined by the following equation between the limits indicated,

$$C_{L_4} = .15 + 1.2\left(\frac{Q_3}{Q_2} - .25\right) \quad . \quad . \quad . \quad . \quad . \quad . \quad . \quad (33)$$

$$\text{for } .25 < \frac{Q_3}{Q_2} < .75$$

If the value for C_{L_4} is computed by Eq. 33 for the case where Q_1 equal zero (i.e. $Q_3/Q_2 = 1$) a value of $C_{L_4} = 1.05$ results. While this value is obtained from extrapolation of the experimental data, and consequently only approximate it is significantly less than the head loss

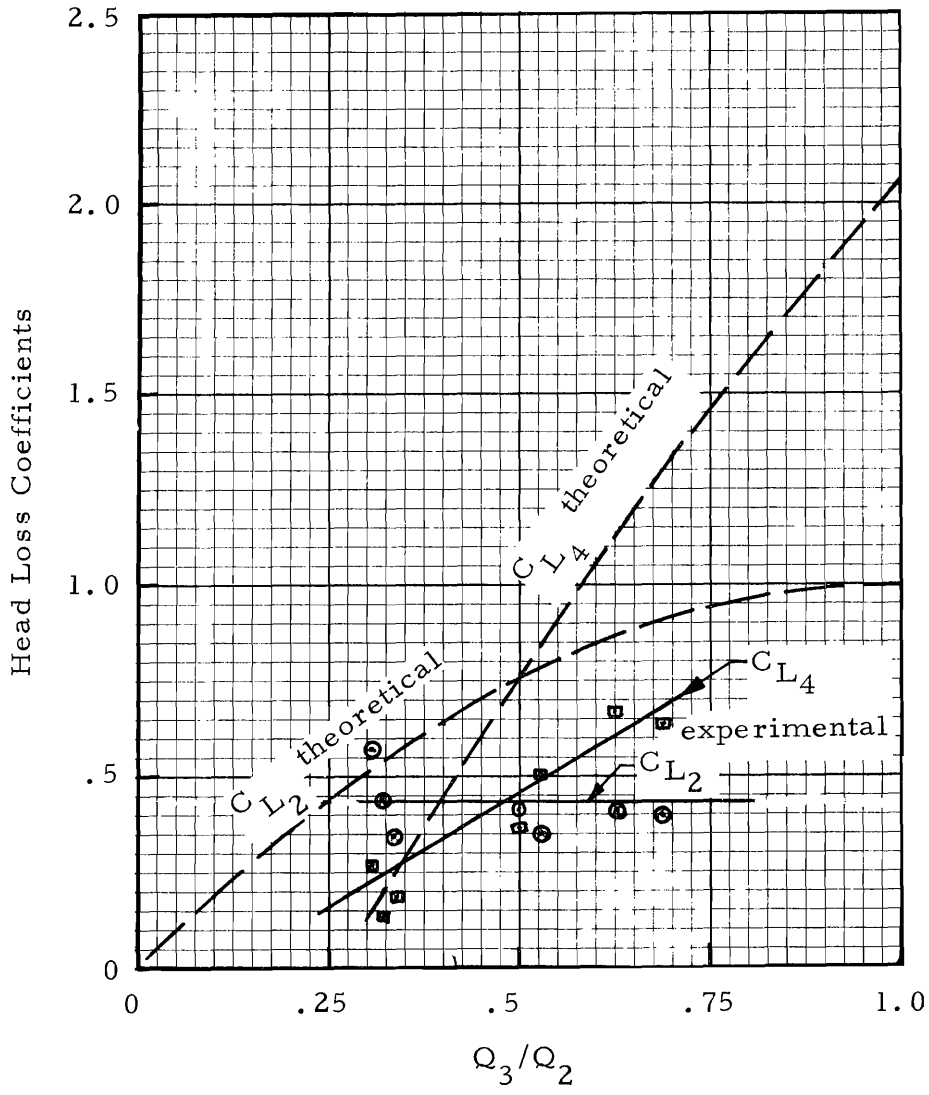

Fig. 17. The variation of head loss coefficients with the ratio of the flow rates Q_3/Q_2, i.e. the flow into the "90°" branch divided by the total outflow.

coefficient obtained from test series No. 5. In test series No. 5 the entire flow was turned through 90^{o}, but the inflow entered one "straight through" branch and left through the "90^{o}" branch, whereas the coefficient of 1.05 computed from Eq. 33 is associated with the flow entering the "90^{o}" branch and leaving through a "straight through" branch. It is not difficult to visualize why smaller head losses result from this latter situation. When the flows enter through the "90^{o}" branch it is turned through 90^{o} by the wall of the tee, whereas when it enters through the "straight through" branch it penetrates into the other "straight through" pipe which is plugged and is forced backward, likely near the pipe walls into the "90^{o}" branch.

CONCLUSIONS

While the tests performed during this study are well-defined, it is surprising how little data are available in the literature to compare the test results with directly. The scatter in the data requires that curve fitting procedures be used to establish relationships between parameters used in describing frictional and other so-called minor head losses. While the scatter in the data is larger than ideally hoped for, the magnitude of the scatter appears to be comparable to the scatter in the data obtained by Blaisdell and Manson (1963), in which they read the manometer with a cathetometer. In the test set-ups used in this study, reading the manometers with a cathetometer was not practical, first because the individual manometers were located along the entire pipe length, and secondly, the holes in the pressure taps were made large so that turbulent pressure fluctuations were transmitted into the manometer causing the mercury columns to fluctuate.

In analyzing the data, however, the results are consistent, and except for the lower flow rates where the error in reading the data is a significant part of the head loss the computed head losses show less scatter than was expected.

The following briefly summarizes the results. PERMASTRAN® pipe is hydraulically smooth within the range of flows used in the tests (i.e. for Reynolds numbers less than approximately 3.5×10^5). From examining the position of the data with respect to the hydraulically smooth energy lines obtained in test series 8 at the highest flow rates of approximately 1500 gpm, it appears for larger Reynolds numbers than 3.5×10^5, the friction factor for the pipe may begin departing from the hydraulically smooth pipe. If this is true, the equivalent roughness, e, for PERMASTRAN® pipe is approximately equal to .000007 ft.

The head loss coefficient due to the 6-inch 90^{o} RING-TITE filament wound elbow is 0.5. When the RING-TITE filament wound 6x6x6-inch tee operates as an elbow, the loss coefficient is approximately three times this large when the flow enters one "straight through" branch and leaves through the "90^{o}" branch, and is probably only twice this large when the flow enters the "90^{o}" branch and leaves through one of the "straight through" branches. When the tee operates to divide an inflow from a "straight through" branch into two outflows, the head loss coefficients, particularly between the inlet branch and the "straight through" outlet branch, are related to Reynolds number (see Fig. 15). When the tee operates to combine two inflows into a single outflow in one "straight through" branch, the head loss coefficients are approximately equal to 0.4 when based on the velocity head in the discharge pipe (see Fig. 16).

REFERENCES

Amorocho, Jaime and Johannas J. DeVries. 1971. Power Losses and Flow Topologies in Converging Manifolds. Journal of the Hydraulics Div., ASCE, Vol. 97, No. HY1, Jan., pp. 81-99.

Blaisdell, Fred W. and Philip W. Manson. 1963. Loss of Energy at Sharp-Edged Pipe Junctions. Technical Bulletin No. 1283, U.S. Dept. of Agriculture, Washington, D. C.

Blaisdell, Fred W. and Philip W. Manson. 1967. Energy Loss at Pipe Junctions. Journal of the Irrigation and Drainage Division, ASCE, Vol. 93, No. IR3, Proc. Paper 5411, Sept., pp. 59-78.

Giesecke, F. E., W. A. Badgett, and J. R. D. Eddy. 1932. Loss of Head in Cast Iron Tees. Texas A & M Bulletin No. 41, College Station.

Hoopes, J. W., et al. 1948. Friction Losses in Screwed Iron Tees. Chemical Engineering Progress, Vol. 44, pp. 691-696.

Jamison, Donald K. and James R. Villemonte. 1971. Junction Losses in Laminar and Transitional Flows. Journal of the Hydraulics Division, ASCE, Vol. 97, No. HY 7, Proc. Paper 8258, July, pp. 1045-1063.

Jeppson, R. W., C. G. Clyde, and C. Kincaid. 1972. Model Study of the Manifold to be used as a Component of the Virginia Electric and Power Company 1970 Extension of Yorktown Power Station. Utah Water Research Laboratory, Utah State University, Logan, Utah, Oct.

Jeppson, R. W., C. G. Clyde, and C. Kincaid. 1973. Hydraulic Tests on Model of Manifold of the Pumps of the 1974 Extension of the Yorktown Power Station With All Combinations of One and Two Branches Taken Out of Operation. Utah Water Research Laboratory, Utah State University, Logan, Utah, Jan.

McNown, J. S. 1953. Mechanics of Manifold Flow. Proceedings, ASCE, Vol. 79.

Olsen, R.M. 1966. Essentials of Engineering Fluid Mechanics. International Textbook Co., Scranton, Penn.

Ruus, Eugen. 1970. Head Losses in Wyes and Manifolds. Journal of the Hydraulics Division, ASCE, Vol. 96, No. HY3, Proc. Paper 7130, March, pp. 593-608.